



**INVESTIGATING THE FUNCTIONAL MECHANISMS  
OF PROTEOLYSIS VIA FTIR AND CD  
SPECTROSCOPY**

**BURÇİN DERSU AÇIKGÖZ**

Master's Thesis

Graduate School  
Izmir University of Economics

Izmir

2022

**INVESTIGATING THE FUNCTIONAL MECHANISMS  
OF PROTEOLYSIS VIA FTIR AND CD  
SPECTROSCOPY**

**BURÇİN DERSU AÇIKGÖZ**

A Thesis Submitted to  
The Graduate School of Izmir University of Economics  
Master's Program in Bioengineering

Izmir  
2022

## ABSTRACT

# INVESTIGATING THE FUNCTIONAL MECHANISMS OF PROTEOLYSIS VIA FTIR AND CD SPECTROSCOPY

Açıkgöz, Burçin Dersu

Master's Program in Bioengineering

Advisor: Asst. Prof. Dr. Burçak Alp

Co-Advisor: Asst. Prof. Dr. Günnur Güler

July, 2022

The enzymatic breakdown of peptide bonds is known as proteolysis and it is a natural process that causes protein polypeptide chain to degrade via cleaving peptide bonds with enzymes. The proteolysis mechanism has significant importance in the pharmaceutical, food and biotechnological sectors. This study aimed to explore the time-dependent molecular alterations of  $\beta$ -casein in the presence of both water-ethanol mixtures and deuterium oxide buffer whereas the molecular alterations of bovine serum albumin (BSA) in water-ethanol mixtures together with the heat treatment throughout the hydrolysis. In this study, the alterations in the secondary structure of  $\beta$ -casein were monitored with Fourier transform infrared (FTIR) spectroscopy while the secondary structure changes of BSA were monitored with Circular Dichroism (CD)

spectroscopy. The applicability of both spectroscopic techniques was attempted to be demonstrated by monitoring spectral changes during tryptic hydrolysis of  $\beta$ -casein and BSA at different temperatures and in different buffer conditions. According to the results of FTIR spectroscopy, the most significant alterations occur in the amide I and amide II regions ( $1700\text{-}1500\text{ cm}^{-1}$ ). Furthermore, as liberated products, the infrared signals of carboxylate groups (asym. stretch vibrations:  $\nu_{\text{as}}(\text{COO}^-)$ ) and NH groups (NH bending vibrations) rise in the range of  $1585\text{-}1613\text{ cm}^{-1}$ . For monitoring the conformational changes of  $\beta$ -casein, advanced data analysis was applied. Furthermore, two-dimensional correlation spectroscopy (2DCOS) analysis and curve-fitting analysis were applied to the FTIR spectroscopy results. CD spectroscopy results revealed that with the addition of ethanol, the structural components of BSA broken down and degraded upon hydrolysis. In conclusion, new methodological approaches were elucidated that will be beneficial to the biotechnological techniques and proteomics studies.

Keywords: Proteolysis, FTIR spectroscopy, CD spectroscopy,  $\beta$ -casein, Bovine serum albumin

# ÖZET

## PROTEOLİZİN FONKSİYONEL MEKANİZMALARININ FTIR VE CD SPEKTROSKOPİSİ İLE İNCELENMESİ

Açıkgöz, Burçin Dersu

Biyomühendislik Yüksek Lisans Programı

Tez Danışmanı: Dr. Öğr. Üyesi Burçak Alp

İkinci Tez Danışmanı: Dr. Öğr. Üyesi Günnur Güler

Temmuz, 2022

Peptit bağlarının enzimatik parçalanması proteoliz olarak bilinir ve protein polipeptit zincirinin enzimlerle peptit bağlarını parçalayarak bozulmasına neden olan doğal bir süreçtir. Proteoliz mekanizması ilaç, gıda ve biyoteknoloji sektörlerinde önemli bir yere sahiptir. Bu çalışmada, hidroliz sırasında sıcaklıkla birlikte hem su-etanol karışımları hem de döteryum oksit tamponu varlığında  $\beta$ -kazeinin zamana bağlı moleküler değişikliklerini incelerken aynı zamanda su-etanol karışımında sığır serum albümininin (BSA) moleküler değişimlerinin incelenmesi amaçlanmıştır. Bu çalışmada  $\beta$ -kazeinin sekonder yapısındaki değişiklikler Fourier dönüşümlü kızılötesi (FTIR) spektroskopisi ile izlenirken, BSA'nın sekonder yapı değişiklikleri Dairesel Dikroizm (CD) spektroskopisi ile incelenmiştir. Her iki spektroskopik tekniğin uygulanabilirliği, farklı sıcaklıklarda ve farklı tampon koşullarında  $\beta$ -kazein ve BSA'nın triptik hidrolizi sırasında spektral değişikliklerin izlenmesiyle gösterilmiştir. FTIR spektroskopisi sonuçlarına göre en önemli değişiklikler amid I ve amid II

bölgelerinde ( $1700-1500\text{ cm}^{-1}$ ) meydana gelmektedir. Ayrıca serbest bırakılan ürünler olarak karboksil gruplarının (asimetrik gerilme titreşimleri:  $\nu_{\text{as}}(\text{COO}^-)$ ) ve NH gruplarının (NH eğilme titreşimleri) IR sinyalleri  $1585-1613\text{ cm}^{-1}$  aralığında yükseldiği gözlemlendi.  $\beta$ -kazeinin konformasyonel değişikliklerinin izlenmesi için gelişmiş veri analizi uygulandı. Ayrıca, FTIR spektroskopisi sonuçlarına 'iki boyutlu korelasyon spektroskopisi (2DCOS) analizi' ve 'curve-fitting analizi' uygulanmıştır. CD spektroskopisi sonuçlarından elde edilen verilerle, etanol varlığında BSA'nın yapısal bileşenlerinin hidroliz sırasında parçalandığı ve bozulduğu ortaya konulmuştur. Sonuç olarak, bu çalışmada biyoteknolojik teknikler ve proteomik çalışmalara fayda sağlayacak yeni metodolojik yaklaşımlar aydınlatılmıştır.

Anahtar Kelimeler: Proteoliz, FTIR spektroskopisi, CD spektroskopisi,  $\beta$ -kazein, Sığır serum albumini

Dedicated to my family...



## ACKNOWLEDGEMENTS

First and foremost, I would like to thank my advisor, Asst. Prof. Dr. Günnur Güler supported me and provided extensive insight into this study. I'm extremely grateful to Asst. Prof. Dr. Günnur Güler for her unconditional guidance that carried me through completing my studies. I would also like to express my appreciation to one of my advisors, Asst. Prof. Dr. Burçak Alp, who assisted me in completing my thesis.

I want to give my deepest appreciation to our laboratory specialist, Zehranur Tekin, who took her time to help me when I had a problem during my experiments and was always there for discussions about anything that I was unsure about.

I am extremely grateful to my mother, Terlan Açıkgöz. Without her great understanding, love and support, it would be impossible for me to complete my thesis. Special thanks to my brother Taylan Dersu Açıkgöz and my father Tayip Sadık Açıkgöz for their continuous understanding and unconditional love.

I would like to extend my sincere thanks to my valuable lab-mates Begümnur Küçükcan, İlayda Akaçin and Şeymanur Ersoy for their unwavering support and faith in me. They made the past two years way more enjoyable and maintained my sanity during the entire time.

I wish to extend my special thanks to my dear friends, Sude Uyulgan, İsmet Kaan Zengin, Berna Karakuyu, Pelin Sayar, Özge Çandarlı and Hatice Döşeme for all their endless support and motivation during this process.

## TABLE OF CONTENTS

ABSTRACT.....	iii
ÖZET.....	v
ACKNOWLEDGEMENTS .....	viii
LIST OF TABLES .....	xi
LIST OF FIGURES .....	xii
LIST OF ABBREVIATIONS .....	xv
CHAPTER 1: INTRODUCTION .....	1
1.1. Proteolysis.....	1
1.1.1. Tryptic Hydrolysis of $\beta$ -casein.....	2
1.1.2. Tryptic Hydrolysis of Bovine Serum Albumin.....	3
1.1.3. The Effect of Ethanol on the Proteolysis Reaction .....	4
1.2. Fourier Transform Infrared Spectroscopy.....	5
1.2.1 General Principles of FTIR Spectroscopy.....	6
1.2.2 Molecular Vibrations .....	7
1.2.3 Protein and Amide Band FTIR Signatures.....	8
1.2.4. H <sub>2</sub> O/D <sub>2</sub> O Buffer Absorption .....	9
1.3. Circular Dichroism Spectroscopy .....	11
1.3.1 General Principles of CD Spectroscopy.....	11
1.3.2 Circular Dichroism Signatures of Proteins .....	13
1.4. The Aim of Study.....	14
CHAPTER 2: MATERIALS AND METHODS .....	16
2.1. Materials.....	16
2.2. Sample Preparation and Proteolysis Reaction for FTIR Spectroscopy Measurements .....	16

2.3 Sample Preparation and Proteolysis Reaction for CD Spectroscopy Measurements .....	18
2.4. Fourier Transform Infrared (FTIR) Spectroscopy .....	19
2.4.1. FTIR Data Processing .....	21
2.5. Circular Dichroism (CD) Spectroscopy .....	21
2.5.1. CD Data Processing .....	22
CHAPTER 3: RESULTS AND DISCUSSION .....	23
3.1. CD Spectroscopy Analysis of BSA Hydrolyzed by Trypsin in Water-Ethanol Medium .....	23
3.2. FTIR Spectroscopy Analysis of $\beta$ -casein Hydrolyzed by Trypsin in Water-Ethanol Medium .....	27
3.2.1. Two-dimensional correlation spectroscopy (2DCOS) analysis of Tryptic Hydrolysis of $\beta$ -casein in Water-Ethanol Medium .....	31
3.2.2. Secondary Structure Analysis of Tryptic Hydrolysis of $\beta$ -casein in Water-Ethanol Medium.....	37
3.3. FTIR Spectroscopy Analysis of $\beta$ -casein Hydrolyzed by Trypsin in Deuterium Oxide Buffer.....	39
CHAPTER 4: CONCLUSION.....	42
REFERENCES.....	44

## LIST OF TABLES

Table 1. Amide I band positions to secondary structure assignment (Barth, 2007). ...	9
Table 2. Experimental data-set for FTIR spectroscopy measurements.....	17
Table 3. Experimental data-set for CD spectroscopy measurements.....	19
Table 4. Asynchronous correlated peaks of $\beta$ -casein digested by trypsin (5000:1 ratio) in 0% EtOH at 25°C for 180 min. ....	33
Table 5. Asynchronous correlated peaks of $\beta$ -casein digested by trypsin (5000:1) in 10% EtOH at 25°C for 180 minutes.....	35
Table 6. Assignment of amide I components and percentages (%) of secondary structure elements of $\beta$ -casein hydrolyzed by trypsin in the absence of ethanol (5000:1 in 0% EtOH) in H <sub>2</sub> O buffer at 25°C (Spectra at t=1 min and t=120 min). ....	38
Table 7. Assignment of amide I components and percentages (%) of secondary structures of $\beta$ -casein digested by trypsin in the presence of 10% Ethanol (5000:1 in 10% EtOH) in H <sub>2</sub> O buffer at 25°C (Spectra at t=1 min and t=120 min). ....	39

## LIST OF FIGURES

Figure 1. The catalytic triad of serine proteases, adapted from (Source: Erez et al., 2009). .....	2
Figure 2. Trypsin's hydrolysis site, adapted from (Source: Berg et al., 2002). .....	3
Figure 3. Scheme of a Michelson interferometer, adapted from (Source: Wang et al., 2012). .....	7
Figure 4. Vibrational modes of (a) H <sub>2</sub> O; (b) CO <sub>2</sub> , adapted from (Source: Langbein and Borri, 2014). .....	8
Figure 5. The infrared absorbance spectrum of water (H <sub>2</sub> O), illustrating the H-O-H bending and O-H stretching vibrations. ....	10
Figure 6. The FTIR absorbance spectra of H <sub>2</sub> O (red) and D <sub>2</sub> O (black). .....	11
Figure 7. Schematic illustration of the optical layout of CD spectroscopy, adapted from (Source: Hoffmann et al., 2016). .....	12
Figure 8. Far-UV CD spectra of secondary structures; $\alpha$ -helix, $\beta$ -sheet, random coil. (Red: $\alpha$ -helix; Green: $\beta$ -sheet; Black: random coil), (Source: Corrêal and Ramos, 2009). .....	14
Figure 9. The work-flow of the study (Created with BioRender.com). .....	15
Figure 10. General view of the FTIR spectroscopy in the transmission mode along with temperature controlling set-up. ....	20
Figure 11. Advanced liquid transmission cell. ....	20
Figure 12. General view of the sample holder set-up in the chamber of the CD spectrometer. ....	22
Figure 13. The far-UV CD spectra recorded at 37°C for 90 min of BSA hydrolyzed by trypsin at a ratio of 5000:1 (S:E) in (A) 0% EtOH; (B) 10% EtOH; (C) 20% EtOH; (D) 40% EtOH. (S:0.5 mg/ml and E:0.0001 mg/ml). .....	24
Figure 14. The far-UV CD spectra were recorded at 37°C for 90 min of (A) Blank BSA in pure water buffer (0% EtOH) and (B) Blank BSA in 10% EtOH. (S:0.25 mg/ml). .....	24
Figure 15. Mean residue ellipticity at 222 nm with respect to time; (A) BSA hydrolyzed by trypsin at a ratio of 5000:1 (S:E) in pure water buffer (0% EtOH) and 10-20-40% EtOH (B) Blank BSA in both 0% EtOH and 10% EtOH at 37°C (plotted	

from Figs. 13 and 14.). To see the alterations all data points have been initialized in the same point (for the y-axis). .....	26
Figure 16. Secondary structure percentages for BSA hydrolyzed by trypsin at the S:E ratio of 5000:1 in 0%, 10%, 20% and 40% EtOH were obtained from the CD spectra at 37°C for t=60 min by using CONTINLL, SELCON3, and CDSSTR methods.....	26
Figure 17. FTIR absorbance spectra of $\beta$ -casein digested by trypsin at the 5000:1 ratio in (A) 0% EtOH (C) 10% EtOH at 25°C for 180 minutes. Difference spectra of (B) 0% and (D) 10% EtOH. Difference spectra were acquired from subtraction of the first spectrum taken at $t_0 = 1$ min from each of the absorbance spectra taken during digestion, $\Delta\text{Absorbance} = \{\text{Digested } \beta\text{-casein (t)}\} - \{\text{Digested } \beta\text{-casein (t}_0 = 1 \text{ min)}\}$ . The arrows demonstrate the intensity changes as a function of time.....	28
Figure 18. (Left) FTIR absorbance spectra of $\beta$ -casein digested by trypsin at a 5000:1 ratio in 0% (Red) and 10% (Black) EtOH at 25°C (t= 120 min); (Right) Difference spectra of the absorbance spectra of $\beta$ -casein digested by trypsin at a 5000:1 ratio in 0% (Black) and 10% (Red) EtOH at 25 °C after 2 hours of hydrolysis (t=120 min).	29
Figure 19. Double difference spectrum of $\beta$ -casein hydrolyzed by trypsin at a ratio of 5000:1 in 0% EtOH and 10% EtOH. Double difference spectrum was acquired from Figure 18 by subtracting the $\Delta\text{Abs}$ of 10% EtOH from $\Delta\text{Abs}$ of 0% EtOH absorbance spectra, $\Delta\text{Absorbance} = \{\Delta\text{Abs of 0\% EtOH (t=120 min)}\} - \{\Delta\text{Abs of 10\% EtOH (t=120min)}\}$ , at 25 °C. ....	30
Figure 20. The intensity changes at 1700 $\text{cm}^{-1}$ , 1545 $\text{cm}^{-1}$ , and at 1613 $\text{cm}^{-1}$ obtained from difference spectra with S:E ratio of 5000:1 ( $\beta$ -casein:Trypsin) in 0% and 10% EtOH at 25°C. (Red: 10% EtOH; Black: 0% EtOH) .....	31
Figure 21. Three-dimensional plot of FTIR absorbance spectrum of $\beta$ -casein digested by trypsin at a 5000:1 ratio in 0% EtOH at 25°C for 180 minutes. ....	32
Figure 22. Synchronous (Left) and asynchronous (Right) 2D FTIR correlation spectrum of $\beta$ -casein digested by trypsin at the S:E ratio of 5000:1 in 0% EtOH at 25°C for 180 minutes. ....	32
Figure 23. A 3D plot of IR absorbance spectra of $\beta$ -casein digested by trypsin (5000:1) in 10% EtOH at 25°C for 180 min. ....	34
Figure 24. Synchronous (Left) and asynchronous (Right) 2D FTIR correlation spectra of $\beta$ -casein digested by trypsin at the 5000:1 ratio in 10% EtOH at 25°C for 180 minutes. ....	34

Figure 25. Curve fit analysis of amide I at t=1 min (Left) and t=120 min (Right) of tryptic hydrolysis of  $\beta$ -casein in the absence of ethanol (5000:1 in 0% EtOH) in H<sub>2</sub>O buffer at 25°C. The envelope bands which are formed by curve fitting are shown in red and the env envelope bands of the original spectra are shown in black color. Before the curve fitting, the corresponding enzyme was subtracted from the hydrolyzed  $\beta$ -casein..... 37

Figure 26. The FTIR difference spectra for  $\beta$ -casein digested by trypsin recorded at 37°C for the S:E ratios of (a) 500:1, (b) 4000:1 and (c) 10000:1 (w/w). The arrows demonstrate the amide changes of  $\beta$ -casein during digestion as a function of time.. 40

Figure 27. The intensity changes acquired from the FTIR-difference spectra (from Fig. 26) with the S:E ratios of 500:1, 4000:1 and 10000:1 (w/w) as a function of time. The content of (a)  $\beta$ -sheets absorbing at 1633 cm<sup>-1</sup>, (b)  $\alpha$ -helix absorbing at 1650 cm<sup>-1</sup> and (c) antisymmetric stretching of free carboxylates (products of proteolysis) absorbing at 1593 cm<sup>-1</sup>..... 41

## LIST OF ABBREVIATIONS

$\mu$ l: microliter

2DCOS: Two-dimensional correlation spectroscopy analysis

BSA: Bovine serum albumin

CD spectroscopy: Circular dichroism spectroscopy

cm: centimeter

DTGS: Deuterated triglycine sulfate

EtOH: Ethanol

FTIR spectroscopy: Fourier transform infrared spectroscopy

H/D Exchange: Hydrogen/Deuterium exchange

IR: Infrared

MCT: Mercury cadmium telluride

min: minute

ml: milliliter

mM: millimolar

PEM: Photoelastic modulator

PMT: Photomultiplier tube

S:E: Substrate to enzyme ratio

SNR: Signal-to-noise ratio

UV: Ultraviolet

$\nu_{as}$ : Antisymmetric stretching

$\nu_s$ : Symmetric stretching

# CHAPTER 1: INTRODUCTION

## *1.1. Proteolysis*

Proteolysis is an enzymatic hydrolysis of a protein where proteins are broken down into smaller polypeptides and/or amino acids. Proteolysis is a natural process and it induces protein polypeptide chain degradation through cleaving peptide bonds with enzymes. The proteolysis process is very crucial for various fields in particular biotechnology, proteomics, biosciences, food and pharmaceutical fields. Proteolysis of specific peptide bonds is vital for a variety of biologically significant processes (digestion, autolysis and blood coagulation) and especially, cellular and molecular control mechanisms. In proteomics, which describes the large-scale study of proteins, proteolysis plays a significant role in the preparation of samples for mass spectroscopy analysis.

During the proteolysis process, proteases can hydrolyze a large polypeptide chain into smaller fragments in particular short peptides and/or amino acids which cleave from the particular peptide bonds of the polypeptides. The serine protease belongs to the protease family and its active site contains histidine, serine and aspartate amino acid residues (Fig. 1) (Polgár, 2005). These amino acid residues create a charge relay that makes the active site of the serine nucleophilic which is accomplished by altering the serine's electrostatic environment. On the other hand, the aspartate is in charge of stabilizing and attracting arginine and lysine which are positively charged (Stryer, 1988).

The serine residue (negatively charged) can attack the peptide bond's carbonyl group which is to be cleaved. This protease class plays a crucial role in proteolysis and involves digestive enzymes (chymotrypsin and trypsin) and numerous proteins that are involved in coagulation (Owen, 2006). The processes and sequence of events in proteolysis for instance monitoring the alterations in the protein secondary structure are not yet fully discovered. Polypeptide chain fragments, whether monomeric or aggregated, offer the enzyme with only restricted access to peptide bonds which is called the masking effect however during proteolysis the accessibility of peptide bonds increases which is called the demasking effect (Güler et al., 2011). In

this thesis, for tryptic hydrolysis of  $\beta$ -casein, enzyme accessibility of peptide bonds throughout proteolysis was investigated.

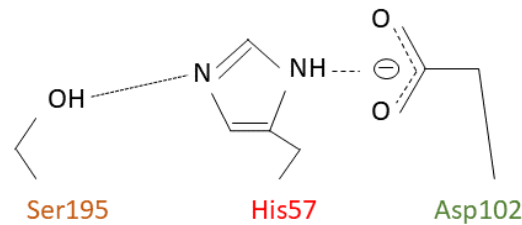


Figure 1. The catalytic triad of serine proteases, adapted from (Source: Erez et al., 2009).

### 1.1.1. Tryptic Hydrolysis of $\beta$ -casein

Casein is the most abundant protein in bovine milk and it constitutes approximately 80% of the whole protein (Atamer et al., 2017). Casein consists of four major protein monomers, named  $\alpha_{S1-}$ ,  $\alpha_{S2-}$ ,  $\beta$ - and  $\kappa$ - caseins (Walstra, 1990). Within the class of caseins,  $\beta$ -casein is the most hydrophobic, consisting of around 45% of the casein in bovine milk (Farrell et al., 2004). Additionally,  $\beta$ -casein is a single polypeptide chain of ~24 kDa acidic protein with 209 amino acids (Grosclaude et al., 1973). It doesn't contain disulfide bonds therefore the tertiary structure of the  $\beta$ -casein is missing. Furthermore, it has a hydrophilic negative N-terminal and a hydrophobic C-terminus region (Holt, 1992). Because of their structural flexibility and abundance of enzyme-accessible peptide links, hydrolysis of caseins by proteases are recognized as easy. In this thesis,  $\beta$ -casein was used because of its nutritional importance in food applications and additionally, it is a promising protein that can be used as a drug carrier (Forrest et al., 2005). Casein offers biodegradability and biocompatibility in oral administration which makes casein a promising protein for encapsulation matrix (Głab and Boratyński, 2017). (Bar-Zeev et al., 2016) have shown that  $\beta$ -casein micelles can function as nano vehicles for target-activated release of hydrophobic drugs and can be useful in the treatment of gastric cancer.

Trypsin is a serine protease in the digestive system which hydrolyzes proteins into small fragments (Polgár, 2005). Trypsin is used in various

biotechnological and pharmaceutical industries (Tavano et al., 2018). It has an optimal temperature value of around 37°C and also a pH value of around 8 (Polgár, 2005). Trypsin's active site is in charge of binding positively charged lysine and arginine (Stryer, 1988). Unless followed by proline, trypsin preferentially cleaves peptides on the carboxyl side of lysine and arginine residues (Fig. 2). Proline's ring structure limits the freedom of rotation, which makes the polypeptide bond more rigid (Manea et al., 2007).

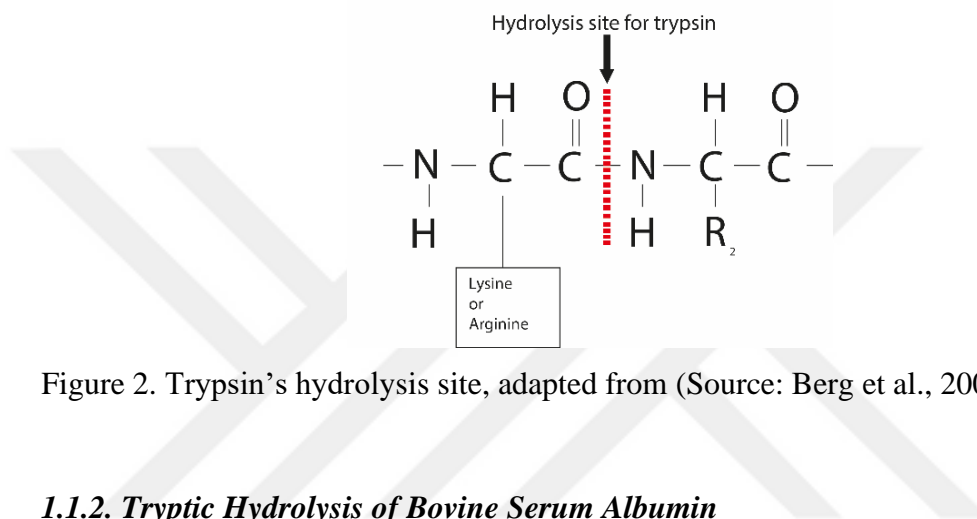


Figure 2. Trypsin's hydrolysis site, adapted from (Source: Berg et al., 2002).

### 1.1.2. Tryptic Hydrolysis of Bovine Serum Albumin

Bovine serum albumin (BSA) is a globular protein and it is the most abundant plasma protein that can be found in the blood circulation system. BSA is used as a protein concentration standard in laboratory studies and various biotechnological applications because of its low cost and tolerance, as well as its ease of preparation. Additionally, the primary biological function of the BSA is to regulate the blood's colloidal osmotic pressure and maintain the pH (Carter and Ho, 1994). BSA is a single polypeptide chain with a molecular weight of 66,430 Da (583 amino acid residues) (Hirayama et al., 1990). In this thesis, BSA was used due to its well-known structure.

Proteolysis of BSA by trypsin has been comprehensively studied and monitored by various techniques, especially with spectroscopic methods in the literature. A study by (Güler et al., 2016), monitored the hydrolysis of BSA with trypsin through circular dichroism (CD) and Fourier transform infrared (FTIR) spectroscopy. In this study, it was proven that both spectroscopic techniques can

monitor the proteolysis in real-time by monitoring the spectral changes along with analysis of the secondary structure of the BSA. It was shown that the secondary structure of the BSA is lost during hydrolysis and is converted to peptide fragments.

### ***1.1.3. The Effect of Ethanol on the Proteolysis Reaction***

Proteolysis' kinetic description involves the detection of the hydrolysis rate constants of peptide bonds in the digested protein however some of the peptide bonds are hidden within proteins or micelles (aggregates) and the interaction with the enzyme is not possible until the steric barriers are removed (Vorob'ev et al., 2015). A major part of proteolysis studies published in the literature were carried out in an aqueous medium and just a few in the water-organic mixture (water-ethanol). Ethanol is commonly used as an organic solvent and also as a protein precipitant. It can affect the hydrogen bonds, hydrophobic and intermolecular electrostatic interactions and cause alterations in protein conformations (Liu et al., 2010).

Trypsin is recognized for being resistant to ethanol additions up to 20% (v/v) and peptide bond specificities' of trypsin were sustained in these conditions (Welinder, 1988). However, the addition of alcohol in proteolysis relies on the concentration of the alcohol, and the studies pointed out that there was no significant effect of alcohol on the hydrolysis of casein, up to 10% ethanol concentrations (Tchorbanov and Iliev, 1993). A study (Tchorbanov and Iliev, 1993) reported that the hydrolysis degree of the casein decreased with the increasing concentration of ethanol. Furthermore, it was revealed that the presence of alcohol made the peptide bonds less sensitive to the enzyme's activity. In another study, (Vorob'ev et al., 2015) performed and monitored proteolysis studies by using  $\beta$ -casein as a substrate in both pure water and water-organic (Ethanol, EtOH) mixtures (0-10-20-40% EtOH (v/v)) by using fluorescence spectroscopy.

Ethanol can affect and denatures the proteins which decreases their solubilities, changes protein-protein interactions and alters the secondary structures (Dufour and Haertl', 1990).  $\beta$ -casein displays amphiphilic properties and the polypeptide chain of this protein involves various unstructured regions which makes the  $\beta$ -casein a very flexible protein whose side and peptide groups are accessible to the solvent (Konnova et al., 2013). Additionally,  $\beta$ -casein forms micelles in aqueous

mixtures (Konnova et al., 2013). A recent study by (Konnova et al., 2013), stated that  $\beta$ -casein was in the monomeric form at low temperatures however upon heating micellar aggregates were formed in the solution. Furthermore, they also reported that the addition of ethanol altered the temperature dependence of protein aggregation. At low concentrations of ethanol, the effect of ethanol is connected with the decrease of intermolecular interactions of the protein and a decrease in micelle formation when the H-bonding of water increases with the presence of ethanol (Vorob'ev et al., 2015). On the other hand, at higher concentrations of ethanol, it is possible that the ethanol can promote the aggregation of the casein.

In the literature, the effects of ethanol on proteins were also investigated using BSA (Vorob'ev et al., 2015; Yang et al., 2022; Yoshikawa et al., 2012). A study by (Yoshikawa et al., 2012), reported that ethanol caused a reduction in the solubility of BSA and also stated that the secondary structure of the BSA was altered. Ethanol is a less polar solvent than water, therefore in the presence of ethanol, comparatively more hydrophobic regions of the protein are exposed which causes the charge density around the protein surface to change (Kundu et al., 2017). Furthermore (Yang et al., 2022) showed the protein protector mechanism of ethanol to understand the interaction between stabilizers and proteins. In this study, human serum albumin (HSA) and ethanol were used as models while IR spectroscopy was used to monitor the secondary structure changes and hydration of HSA.

## ***1.2. Fourier Transform Infrared Spectroscopy***

Infrared (IR) spectroscopy studies the interaction between matter and infrared radiation which examines the IR region of the electromagnetic spectrum. In IR spectroscopy, a sample is irradiated with infrared light and reflected or transmitted light is measured. IR light absorption stimulates the rotational and vibrational levels of macromolecules' functional groups (Barth, 2007). The resulting spectrum demonstrates the molecular absorption which shows the sample's molecular fingerprint.

FTIR spectroscopy is a vibrational spectroscopic method that is used in clinical laboratories as a quantitative analysis tool for comprehensive chemical analysis of the sample solutions. Furthermore, the FTIR method provides direct information on the structures and biochemical components of biological samples

(Finlayson et al., 2019). It provides rapid, nondestructive, non-invasive, label-free, simple and also cost-effective chemical compound analysis intending to obtain a molecular fingerprint of the samples relying on vibrational transitions of intermolecular bonds via infrared light (Finlayson et al., 2019). Another benefit of using the FTIR technique to analyze the samples is that the sample volumes can be as small as 5  $\mu\text{L}$  or lower.

### ***1.2.1 General Principles of FTIR Spectroscopy***

FTIR spectrometer involves an interferometer instead of a dispersive monochromator, which enables the detection of simultaneous wavelength. Among the FTIR interferometers, the Michelson interferometer design is the most commonly used type (Fig. 3) (Wang et al., 2012). The interferometer includes a beam splitter, source, detector, a fixed mirror and a moving mirror. The most common source is a Globar source which is used as a thermal light source for IR spectroscopy. In the course of the measurement, the IR light enters the interferometer and is directed at the beam splitter. After that, the beam is split and directed at a fixed and moving mirror. Then, the beam is recombined which causes interference and is directed at the sample material. After the light is directed through the sample, it enters the detector. The detector transduces the light intensity it receives into an electrical signal. The most frequently used detectors are the deuterated triglycine sulfate (DTGS) detectors and the mercury cadmium telluride (MCT) detectors (Subramanian and Rodriguez-Saona, 2009). The DTGS is a thermal detector and can be used for most protein spectroscopic measurements. In the DTGS detector, the signal is generated in response to the temperature change which is caused by IR light absorption. DTGS detectors can be operated at room temperature. The MCT is a semiconductor detector. In the MCT detector, the electrons are excited by the absorption of IR radiation. The sensitivity of the MCT detectors is higher than the DTGS detectors, therefore the MCT detectors offer a spectrum with a higher signal-to-noise ratio (SNR). SNR can be described as the ratio of the height of a band to the height of the noise at some point in the spectrum and it is proportional to the square root of the scan numbers. Hence, by adding many scans, the SNR can be increased. Furthermore, the data collection is faster in MCT detectors than in the DTGS.

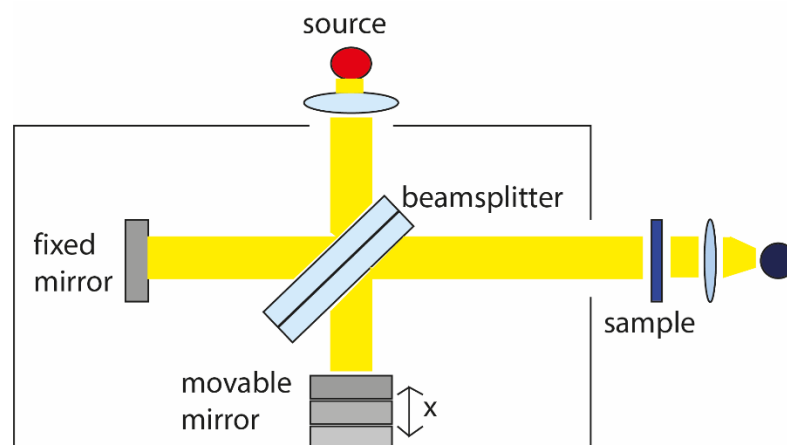


Figure 3. Scheme of a Michelson interferometer, adapted from (Source: Wang et al., 2012).

Furthermore, FTIR spectroscopy is a technique for identifying proteins and peptides. The repeating amino acid building blocks which make up the backbone of proteins generate a variety of unique infrared absorption bands that contains both chemical and structural information. Thus, FTIR spectroscopy is comprehensively used to examine and quantify the secondary structures of the proteins.

### 1.2.2 Molecular Vibrations

The samples are examined using an infrared beam which stimulates the intermolecular bond vibrations that will selectively absorb certain infrared wavelengths according to Beer-Lambert's law depending on the particular molecular bonding environment (Baker et al., 2014).

Molecular motions appear as vibrational, translational and rotational. Additionally, there are mainly two types of vibration modes; stretching and bending. These stretching vibrations can be symmetric ( $\nu_s$ ) or anti-symmetric ( $\nu_{as}$ ). Both symmetric and asymmetric stretching vibrations of the non-linear water molecule ( $H_2O$ ) absorb IR light due to the dipole moment changes (Fig. 4a). Since all vibrational modes of the water create a change in the dipole moment, it is defined as IR-active. Carbon dioxide ( $CO_2$ ), which is a linear molecule, symmetrical stretching vibrations do not absorb IR light (IR-inactive) since this vibration does not cause a dipole moment change (Fig. 4b). However, the asymmetric stretching vibrations absorb IR light due to the dipole moment changes.

Stretching vibrations can be described as the changes in the bond length while bending vibrations are the changes in the angles between two bonds. Bending modes can be divided into 4 groups; in-plane rocking, in-plane scissor bending, out-of-plane wagging and twisting.

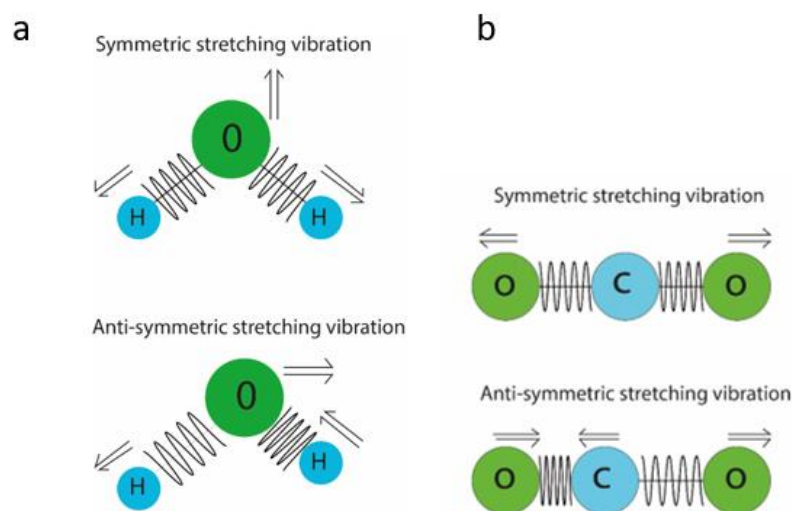


Figure 4. Vibrational modes of (a) H<sub>2</sub>O; (b) CO<sub>2</sub>, adapted from (Source: Langbein and Borri, 2014).

### 1.2.3 Protein and Amide Band FTIR Signatures

In the mid-IR region, the amide I and amide II bands shows the most pronounced protein vibrational modes and these bands reveal the secondary structure of the proteins along with their dynamics and flexibility (Barth, 2007). The amide I band which absorbs near 1650 cm<sup>-1</sup>, mainly arises from stretching vibrations of the C=O with a small contribution of stretching vibrations of the CN molecule. The amide II band which absorbs around 1550 cm<sup>-1</sup>, arises from the N-H bending and also C-N stretching vibrations (Barth, 2007). The vibration of the amide I band is barely affected by the side chain nature however it relies on the backbone's secondary structure so the amide I vibration generally is used for the analysis of the protein secondary structures. In addition to this, the amide II band also provides the secondary structure information and the prediction of secondary structure can be made with this band alone (Barth, 2007). Additionally, within the amino acids only Aspartic acid (Asp), Glutamine acid

(Glu), Asparagine (Asn), Glutamine (Gln), Lysine (Lys), Arginine (Arg), Tyrosine (Tyr), Phenylalanine (Phe) and Histidine (His) have important absorbance within 1750-1480  $\text{cm}^{-1}$  (Barth, 2000).

Proteins' conformational alterations and secondary structural features like  $\alpha$ -helices,  $\beta$ -sheets, turns, and disordered (random coils) display frequency alterations in the amide bands (Table 1). Due to broad bands at near wavenumbers,  $\alpha$ -helix and random coil structures overlap in the amide I band of the  $^1\text{H}_2\text{O}$  buffer, whereas  $\beta$ -sheets show different features in the amide I region.

Table 1. Amide I band positions to secondary structure assignment (Barth, 2007).

Secondary Structure	Band position in $^1\text{H}_2\text{O}$ ( $\text{cm}^{-1}$ )	Band position in $^2\text{H}_2\text{O}$ ( $\text{cm}^{-1}$ )
$\alpha$ -helix	1654	1652
$\beta$ -sheet (weak)	1684	1679
$\beta$ -sheet (strong)	1633	1630
Turns	1672	1671
Disordered	1654	1645

#### 1.2.4. $\text{H}_2\text{O}/\text{D}_2\text{O}$ Buffer Absorption

The extra amount of water that is found in biological fluids absorbs too much IR light in the middle IR region and as a result, it becomes difficult to obtain accurate information about the content of the sample (Finlayson et al., 2019). The absorption of water occurs because of the strong O-H absorption which is caused by the H-O-H bending and O-H stretching vibrations. The O-H stretching vibrations, which is the changing in bond length, can be observed at 3315  $\text{cm}^{-1}$  whereas the H-O-H bending vibrations, changing in the bond angle, can be observed at around 1645  $\text{cm}^{-1}$  (Fig. 5) (Barth and Zscherp, 2002).

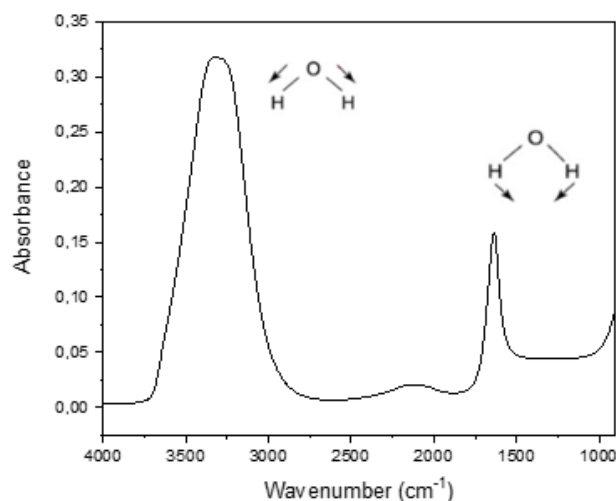


Figure 5. The infrared absorbance spectrum of water (H<sub>2</sub>O), illustrating the H-O-H bending and O-H stretching vibrations.

The absorbance of water in the mid-IR region which overlaps with the amide I band of proteins can create difficulties during the measurement of the aqueous solutions. The H-O-H bending vibrations of H<sub>2</sub>O absorbs very strongly at around 1645 cm<sup>-1</sup> and overlap with the amide I, thus, D<sub>2</sub>O can be used to overcome this problem. In this thesis, it has been also studied with a D<sub>2</sub>O buffer for some experimental dataset groups to overcome the absorbance of the H<sub>2</sub>O in the amide I region (1700-1600 cm<sup>-1</sup>). Deuterium oxide, also known as heavy water, can be defined as a form of water that is composed of oxygen and deuterium which is a heavier isotope of hydrogen. The presence of deuterium gives the water different physical and chemical properties due to the increase in mass. As illustrated in Figure 6, with the H/D (Hydrogen/Deuterium) exchange, the amide I (by 2-10 cm<sup>-1</sup>) and amide II (by ~100 cm<sup>-1</sup>) bands shift in the direction of lower wavenumbers due to the heavy water (Güler et al., 2016).

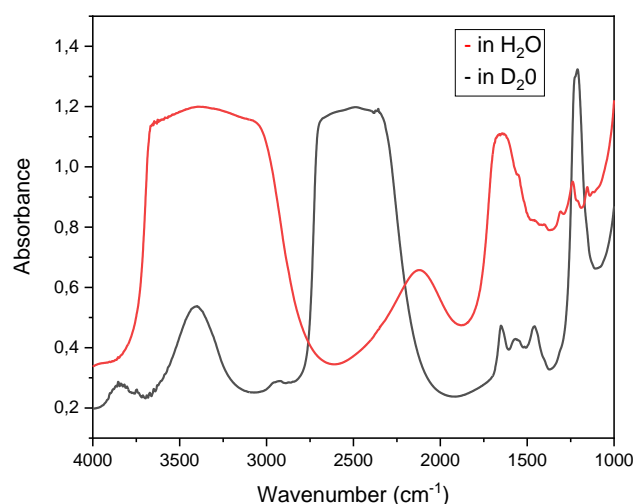


Figure 6. The FTIR absorbance spectra of H<sub>2</sub>O (red) and D<sub>2</sub>O (black).

### 1.3. Circular Dichroism Spectroscopy

Circular Dichroism (CD) spectroscopy is an analytical tool for identifying chirality in molecules by measuring their optical activity. CD spectroscopy measures the difference in absorption of left-handed and right-handed circularly polarized light. It has been commonly used for macromolecular structure elucidation, in particular for proteins and nucleic acids. The high sensitivity of CD to conformational changes makes it a great method for examining the effects of alterations in conditions such as; temperature, pH and ionic strength (Martin and Schilstra, 2008).

#### 1.3.1 General Principles of CD Spectroscopy

The light produced by a CD is linearly polarized before being transformed into circularly polarized light. Unpolarized light is first sent via a polarizer, which aligns the crystal axes and molecules' orientation. A photoelastic modulator is used to transform linearly polarized light into circularly polarized light (PEM). After that, PEM is used to convert linear polarized light into alternating left and right polarized light. The difference in absorption between the two polarizations is measured using a Photomultiplier Tube (PMT) (Fig.7).

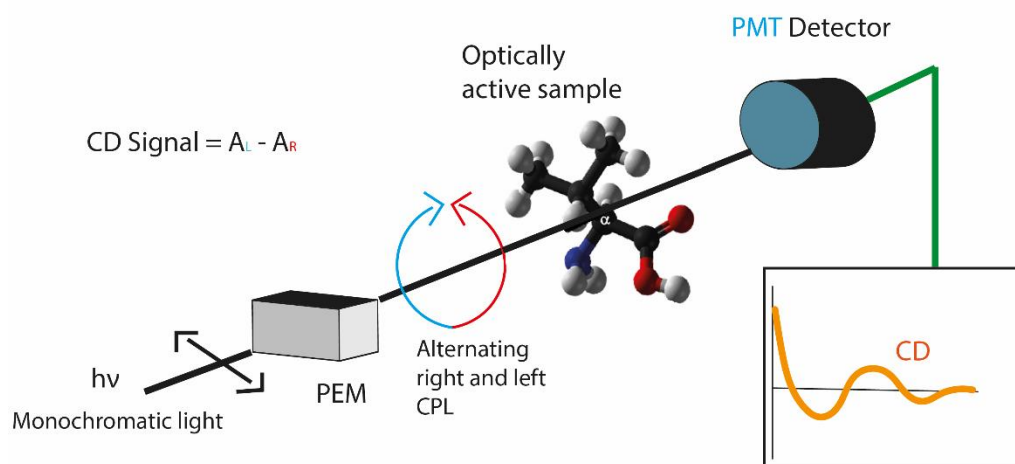


Figure 7. Schematic illustration of the optical layout of CD spectroscopy, adapted from (Source: Hoffmann et al., 2016).

The xenon arc lamp in the CD spectrometer produces a substantial amount of UV radiation. When this radiation interacts with oxygen molecules, ozone is created and ozone oxidizes the surface of the mirrors on the instrument, reducing their reflectivity and efficacy in focusing light through the monochromator which lowers the signal to noise (S/N) ratio. The CD data are generally reported as degrees of ellipticity ( $\theta$ ). Molar ellipticity ( $[\theta]$ ) can be defined as CD corrected for concentration and the unit of molar ellipticity is reported as  $\text{deg cm}^2 \text{dmol}^{-1}$  (Martin and Schilstra, 2008). To calculate the molar ellipticity of a protein sample, the concentration of the sample, path length of the cell and the mean residual weight (molecular weight of amino acids in the protein sample) must be known.

Furthermore, oxygen is absorbed in the UV zone. So, by purging the monochromator with nitrogen, the mirrors retain their reflectivity and lifespan while also reducing oxygen absorption, allowing sample data to be acquired further into the far-UV.

### 1.3.2 Circular Dichroism Signatures of Proteins

To be optically active, a molecule must be chiral or asymmetric, since they absorb left and right-handed polarized light differently. Biological macromolecules including proteins and DNA include optically active components. CD spectroscopy of proteins can be divided into two regions; far UV and near UV. The far UV CD data is collected from ~190 to 250 nm whereas the near UV CD data is collected from 250 to 300 nm (Rodger, 2018). The near UV region is generally used for determining the concentration of the protein (Hoffmann et al., 2016). Secondary structures of protein samples can be observed in the far UV CD region (Hoffmann et al., 2016). The far UV CD spectrum is sensitive to the secondary protein structures such as  $\alpha$ -helix,  $\beta$ -sheet, and random coil (Fig. 8). The  $\alpha$ -helical proteins have a positive band at 193 nm and negative bands at 222 nm and 208 nm (Holzwarth and Doty, 1965).

The spectra of  $\alpha$ -helix include the signal of  $\pi \rightarrow \pi^*$  transition which is divided into two because of the exciton coupling. This transition is mainly responsible for the positive band at 190 nm and a negative band at 208 nm which is a characteristic of the  $\alpha$ -helix spectra. Additionally,  $\pi \rightarrow \pi^*$  transition is responsible for a positive band at 198 nm,  $\beta$ -sheet characteristics. The  $n \rightarrow \pi^*$  transition is responsible for a negative band at 222 nm which is a characteristic of the  $\alpha$ -helix CD spectra and additionally at 218 nm which comes from the  $\beta$ -sheet spectra (Corrêal and Ramos, 2009). On the other hand, the CD spectra for  $\beta$ -sheet proteins have a positive band between 195 nm to 200 nm and a negative band between 210 nm to 222 nm. Since the  $\beta$ -sheet proteins can appear in parallel, antiparallel or mixed conformations, their spectra can be more diversified than  $\alpha$ -helical proteins (Corrêal and Ramos, 2009). The CD spectra of random coil protein have a negative band around 200 nm.

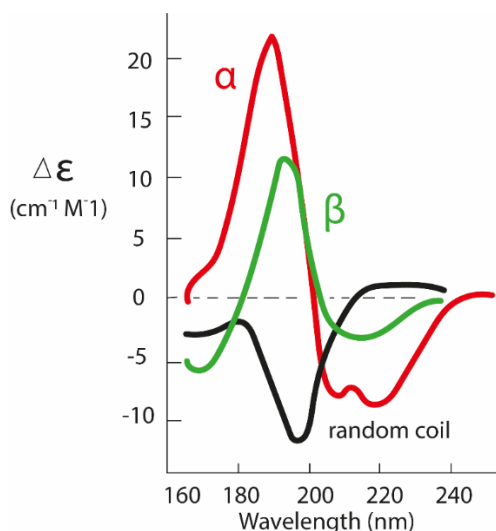


Figure 8. Far-UV CD spectra of secondary structures;  $\alpha$ -helix,  $\beta$ -sheet, random coil. (Red:  $\alpha$ -helix; Green:  $\beta$ -sheet; Black: random coil), (Source: Corrêal and Ramos, 2009).

#### 1.4. The Aim of Study

This thesis aimed to investigate the time-dependent structural changes of selected proteins (substrates) in the presence of deuterium oxide and water-ethanol mixtures during hydrolysis. Herein, it is hoped that this study will lead to the development of new methodological techniques that will be beneficial for proteomics, the food and pharmaceutical industries, and biotechnological applications. The functional mechanisms of proteolysis are elucidated in detail by using FTIR and CD spectroscopic techniques.

Another objective was to develop a quantitative model of proteolysis based on spectral changes, using different substrates (native and gently modified substrates with ethanol) and enzymes. This thesis aims to catch the burst phase of proteolysis by lowering the substrate to enzyme ratio and slowing the hydrolysis process by decreasing the temperature. Furthermore, alterations in the secondary structure of proteins and the sequence of events were investigated in real-time during the proteolysis process, which would allow a detailed study of the proteolysis mechanisms of the proteins. The workflow and stages in this thesis are summarized in Figure 9.

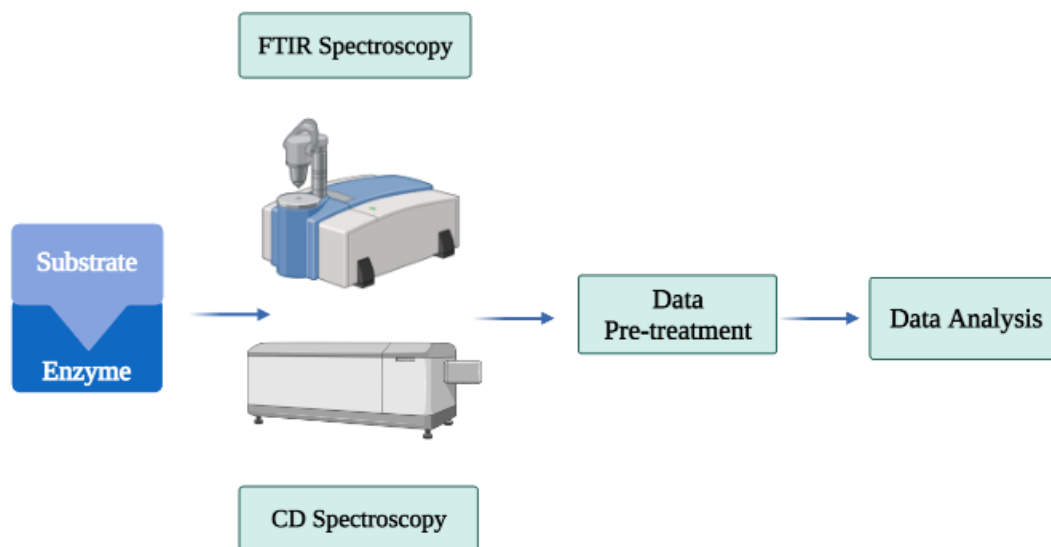


Figure 9. The work-flow of the study (Created with BioRender.com).

## CHAPTER 2: MATERIALS AND METHODS

### *2.1. Materials*

Albumin from bovine serum (BSA) (Sigma-Aldrich, A7906) and  $\beta$ -casein (Sigma-Aldrich, C6905) from bovine milk was used as substrates while trypsin (Sigma-Aldrich, T1426) from bovine pancreas was used as an enzyme. Substrate and enzyme solutions were used without further treatment. The prepared samples of substrate-enzyme solutions were stored at proper temperatures. D<sub>2</sub>O (99.9%) and ethanol (99.9%) were purchased from Sigma-Aldrich.

Additionally, all samples were freshly prepared and used during the experiments in a few days. Sample solutions were prepared by dissolving the freeze-dried powder in potassium phosphate (KPi) buffer. Proper amounts of acid and base salts which are K<sub>2</sub>HPO<sub>4</sub> and KH<sub>2</sub>PO<sub>4</sub> were mixed in both water-ethanol mixtures (pH 7.9) and deuterium oxide (pD 7.9), separately.

### *2.2. Sample Preparation and Proteolysis Reaction for FTIR Spectroscopy Measurements*

Table 2 summarizes the experimental datasets of FTIR spectroscopy and it illustrates the experimental conditions and parameters which are substrate to enzyme ratio (S:E), temperature, buffer conditions and pH.  $\beta$ -casein was used as a substrate while trypsin was used as an enzyme for the FTIR spectroscopy measurements. All protein solutions ( $\beta$ -casein) were prepared by dissolving the freeze-dried powder in potassium phosphate buffer separately in deuterium oxide buffer, pure water buffer and water-ethanol mixtures at various concentrations of substrate and enzyme.

$\beta$ -casein was adjusted to a concentration of 50 mg/ml (initial concentration) for the FTIR spectroscopic measurements that were prepared in deuterated 20 mM KPi D<sub>2</sub>O buffer (pD 7.9). The deuterated samples were equilibrated for 24 hours in 20 mM D<sub>2</sub>O buffer at +4 °C. All proteolytic FTIR experiments that were prepared in deuterium oxide (20 mM, pD 7.9) buffer were performed at a constant substrate concentration of 50 mg/ml (initial concentration) and analyzed at the temperature of 37°C for 90 minutes. The stock trypsin solution (0.1 mg/ml) was prepared under the same

conditions and was diluted to get the required concentrations. The  $\beta$ -casein to trypsin ratio was 500:1, 4000:1 and 10000:1 (w/w). Blank solutions of  $\beta$ -casein (25 mg/ml) were recorded without the trypsin addition. To initiate the proteolysis process, equal amounts of substrate (50  $\mu$ l) and enzyme (50  $\mu$ l) solutions were mixed within an eppendorf tube.

Additionally,  $\beta$ -casein samples were also prepared in both pure water buffer and water-ethanol mixtures.  $\beta$ -casein was adjusted to a concentration of 50 mg/ml (initial concentration) and prepared in 10 mM potassium phosphate buffer pH 7.9 with pure water buffer (0% EtOH) and with the addition of EtOH (10% v/v) at a temperature of 25°C for 180 minutes.  $\beta$ -casein to trypsin ratio was 5000:1 (w/w). The trypsin stock solution (0.1 mg/ml) was prepared under the same conditions and was diluted to get the required concentrations.

Table 2. Experimental data-set for FTIR spectroscopy measurements.

Substrate:Enzyme	Buffer Condition	Substrate:Enzyme Ratio	Temperature
$\beta$ -casein: Trypsin	20 mM KPi D <sub>2</sub> O	- Blank $\beta$ -casein (25 mg/ml)	37°C
	Buffer pH 7.9 (deuterated)	- 500:1 $\beta$ -casein (50 mg/ml) + Trypsin (0.1 mg/ml)	
		- 4000:1 $\beta$ -casein (50 mg/ml) + Trypsin (0.0125 mg/ml)	
		- 10000:1 $\beta$ -casein (50 mg/ml) + Trypsin (0.005 mg/ml)	
$\beta$ -casein: Trypsin	(With and without ethanol)	(Only one S:E ratio was selected)	25°C
	- 10 mM KPi H <sub>2</sub> O Buffer pH 7.9 + 0% EtOH (no ethanol)	- 5000:1 $\beta$ -casein (50 mg/ml) + Trypsin (0.01 mg/ml)	
	- 10 mM KPi H <sub>2</sub> O Buffer pH 7.9 + 10% EtOH		

### ***2.3 Sample Preparation and Proteolysis Reaction for CD Spectroscopy Measurements***

Table 3 summarizes the experimental groups of CD spectroscopy and it demonstrates the experimental conditions and parameters which are substrate to enzyme ratio (S:E), temperature, buffer conditions and pH. BSA was used as a substrate while trypsin was used as an enzyme for the CD spectroscopic measurements.

To start the proteolytic reaction, the substrate (BSA) and trypsin solutions were mixed in an eppendorf tube at equal amounts of volumes (substrate: 350  $\mu$ l and enzyme: 350  $\mu$ l), then instantly transferred to the CD cuvette. A 700  $\mu$ l of the sample solutions were pipetted into the CD cuvette (0.2 cm pathlength) and the CD cuvettes were capped and sealed during all experiments to prevent sample evaporation.

The BSA to trypsin ratio of the samples prepared in pure water buffer and water-organic mixtures was 5000:1 (S:E). The concentration of the protein solutions was adjusted to 0.5 mg/ml (initial concentration) and dissolved by stirring in 10 mM potassium phosphate buffer without (pure water, 0% EtOH) or with the addition of EtOH (10, 20 and 40% EtOH v/v) at pH 7.9. Blank solutions of the proteins (0.25 mg/ml) were recorded and analyzed both in the 0% EtOH (pure water buffer) and 10% EtOH buffer. Prepared sample solutions of BSA were analyzed at 37°C for 90 minutes.

Table 3. Experimental data-set for CD spectroscopy measurements.

Substrate:Enzyme	Buffer Condition	Substrate:Enzyme Ratio	Temperature
BSA:Trypsin	(With and without ethanol)	(Only one S:E ratio was selected)	37°C
	- 10 mM KPi H <sub>2</sub> O Buffer pH 7.9 + 0% EtOH (no ethanol)	- 5000:1 BSA (0.5 mg/ml) + Trypsin (0.0001 mg/ml)	
	- 10 mM KPi H <sub>2</sub> O Buffer pH 7.9 + 10% EtOH	- Blank BSA (0.25 mg/ml) in 0% EtOH	
	- 10 mM KPi H <sub>2</sub> O Buffer pH 7.9 + 20% EtOH	- Blank BSA (0.25 mg/ml) in 10% EtOH	
- 10 mM KPi H <sub>2</sub> O Buffer pH 7.9 + 40% EtOH			

#### 2.4. Fourier Transform Infrared (FTIR) Spectroscopy

PerkinElmer UATR Two FTIR spectrometer which is equipped with a DTGS detector was used to record and monitor the FTIR spectra in the transmission mode. In the transmission mode, the IR light does not pass through a crystal, it passes directly into the sample. A demountable thin layer of infrared CaF<sub>2</sub> (Calcium Fluoride) windows were used during all of the FTIR measurements (Fig. 10). Solutions of samples were pipetted onto (2.5 µl of the sample solution) window cells and before sealing the windows together, they were coated with PTFE paste to prevent the evaporation of the sample solution. The path length of the IR window was 14 µm.

Furthermore, to keep the temperature of the sample constant and stable at fixed temperatures, a circulating water system that has a microcomputer-controlled cryogenic thermostatic bath (LabART) was used during the experiments (Fig. 10). The sample holder set-up in the FTIR spectrometer chamber was changed to make it compatible with the temperature controlling set-up system, which enables real-time and fixed temperature spectral recording during the hydrolysis (Fig. 10). It is an advanced liquid transmission cell with detachable, sealed, static configurations that allow liquid samples to be evaluated at temperatures higher or lower than ambient (Fig. 11).

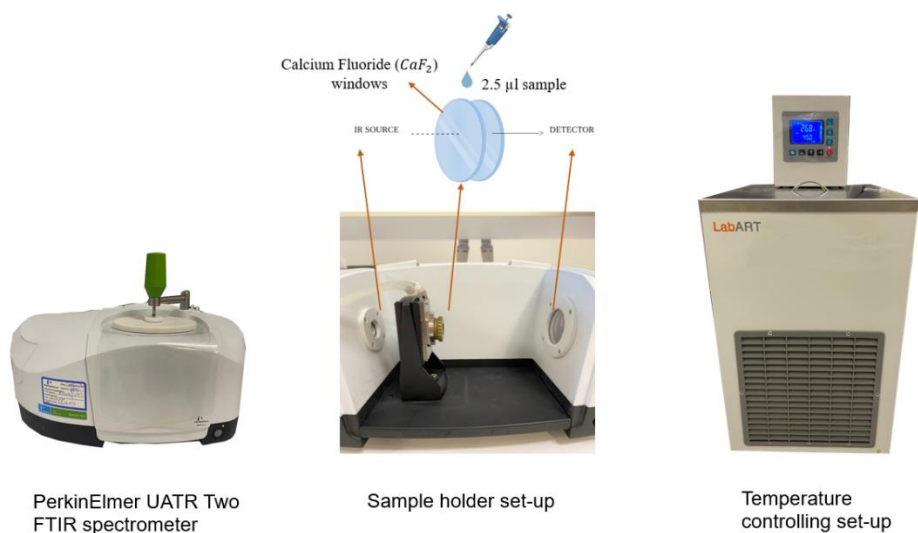


Figure 10. General view of the FTIR spectroscopy in the transmission mode along with temperature controlling set-up.

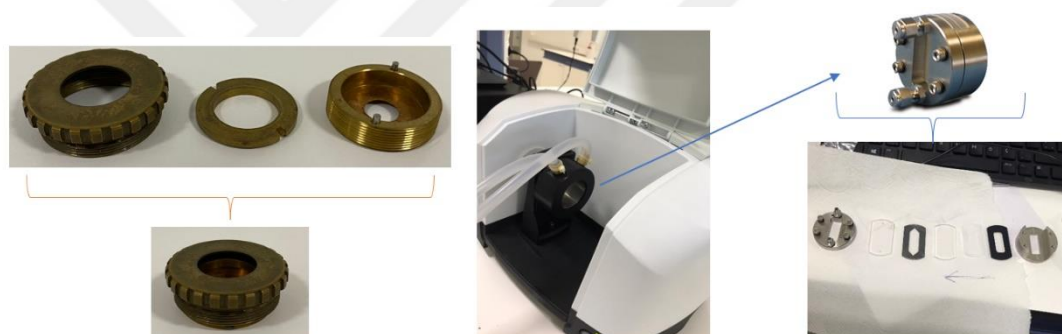


Figure 11. Advanced liquid transmission cell.

The spectra were recorded in the range of  $4000-1000\text{ cm}^{-1}$  with a resolution of  $4\text{ cm}^{-1}$  and 8 scans for 180 minutes at various periods. Before each measurement air was taken as a background. The buffer and enzyme mixtures were also measured in the same conditions to serve as a reference for correcting the sample spectra from buffer and enzyme absorption.

### **2.4.1. FTIR Data Processing**

All of the FTIR spectroscopy measurement results were analyzed with "OPUS 7.0" software (Bruker, Germany). As described in (Güler et al., 2016), the FTIR spectra were buffer-subtracted, baseline-corrected, and area-normalized in the 1725-1375  $\text{cm}^{-1}$  range. Afterward, FTIR difference spectra were calculated by subtracting the first spectrum collected at  $t_0=1$  minute from each absorbance spectrum.

Additionally, two-dimensional correlation spectroscopy (2DCOS) analysis was used to determine the order of events during proteolysis. 2DCOS analysis has been extensively used for analyzing the spectroscopic data which improves the resolution of the spectra and detection of the sequential order of events by the rules of 'sequential order' (de la Arada et al., 2012; Lu et al., 2015; Noda, 2007; Noda and Ozaki, 2005). 2DCOS provides cross-correlation analysis of the spectral series regarding a modulation variable. Additionally, 2DCOS can generate 2D correlation maps. The synchronous map provides correlations between all spectral bands changing during the experiment whether or not they decrease or increase with each other while the asynchronous correlation map shows the wavenumber that changes at different rates and additionally it involves information about the sequence of event occurrence (Lu et al., 2015; Noda and Ozaki, 2005).

Furthermore, curve-fitting analysis was carried out to estimate the content of protein secondary structures which is embedded in the OPUS 7.0 software. The curve-fitting analysis was performed for the amide I region (1700-1600  $\text{cm}^{-1}$ ) after corresponding buffer correction to find out the percentages of each secondary structural elements such as  $\alpha$ -helix,  $\beta$ -sheet, turn/loop, random coils, as described in (Güler et al., 2016).

### **2.5. Circular Dichroism (CD) Spectroscopy**

The CD spectra (185-260 nm) were recorded at 1 nm intervals with 8 accumulations at a scan speed of 100 nm/min for 90 minutes at various time intervals using a JASCO J-1500 spectrometer. The CD data were then converted to the mean residue ellipticity ( $\text{deg cm}^2 \text{dmol}^{-1}$ ), which was computed using the concentration of the protein, pathlength of the CD cuvette and molecular weight of the protein. A circulating water system was used to keep the sample temperature stable at a fixed

temperature. The temperature of the samples was controlled by using a circulating water system (Jasco CTU-100). Figure 12 illustrates the sample holder set-up system of the CD spectrometer.

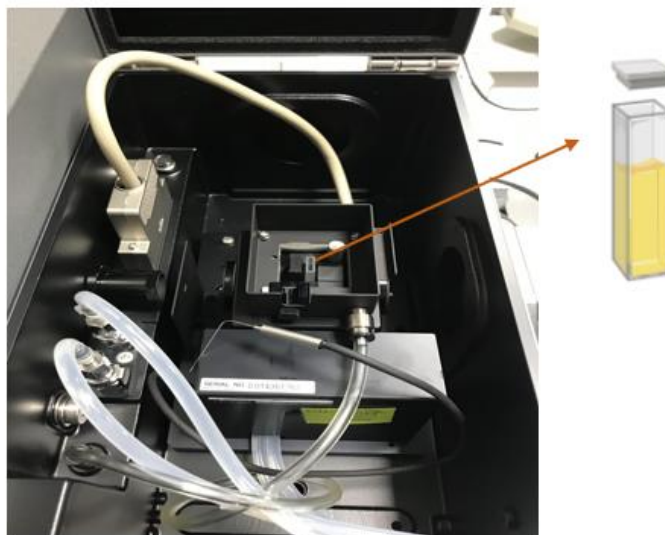


Figure 12. General view of the sample holder set-up in the chamber of the CD spectrometer.

### ***2.5.1. CD Data Processing***

The analysis of protein secondary structure was performed with a software program called CDPro which contains CONTINLL, SELCON and CDSSTR methods, as explained in (Güler et al., 2016; Güler et al., 2011). The analysis of the CD spectrum with CDPro provides secondary structural elements which are distorted and regular  $\alpha$ -helix, distorted and regular  $\beta$ -sheet, unordered and turn structures (Sreerama and Woody, 2000). These three methods involve the protein reference sets along with well-known 3D structures obtained from X-ray diffraction studies. The content of secondary structures of the proteins was estimated within the range of 185-240 nm via a 42-protein reference set (Sreerama and Woody, 2000). To get the total  $\alpha$ -helix and  $\beta$ -sheet content, the percentage values of the distorted and regular structures were added up, separately. The values of all three methods were averaged for the final result of secondary structural content.

## CHAPTER 3: RESULTS AND DISCUSSION

### *3.1. CD Spectroscopy Analysis of BSA Hydrolyzed by Trypsin in Water-Ethanol Medium*

The BSA to trypsin ratio of the samples prepared in pure water buffer and the water-ethanol medium was 5000:1 (S:E, Substrate:Enzyme). The BSA concentration was adjusted to 0.5 mg/ml and dissolved by stirring in 10 mM potassium phosphate buffer without (pure water, 0% EtOH) and with EtOH (10, 20 and 40% EtOH v/v). The CD spectra (185-260 nm) were recorded at 1 nm intervals with 8 accumulations at a scan speed of 100 nm/min for 90 minutes at various time intervals by using the JASCO J-1500 spectrometer. To catch the burst phase of the proteolysis reaction, the CD spectra were recorded with 2 accumulations for the first 6 minutes. After the measurement, the CD data were converted to the mean residue ellipticity ( $\text{deg cm}^2 \text{dmol}^{-1}$ ).

To investigate the ethanol effect on the tryptic hydrolysis of BSA, the experiments were performed with various ethanol concentrations. As comprehensively explained in the Introduction section, ethanol can be described as a protein precipitant and it is anticipated that ethanol does not cause permanent denaturation of plasma proteins such as BSA protein (Yoshikawa et al., 2012).

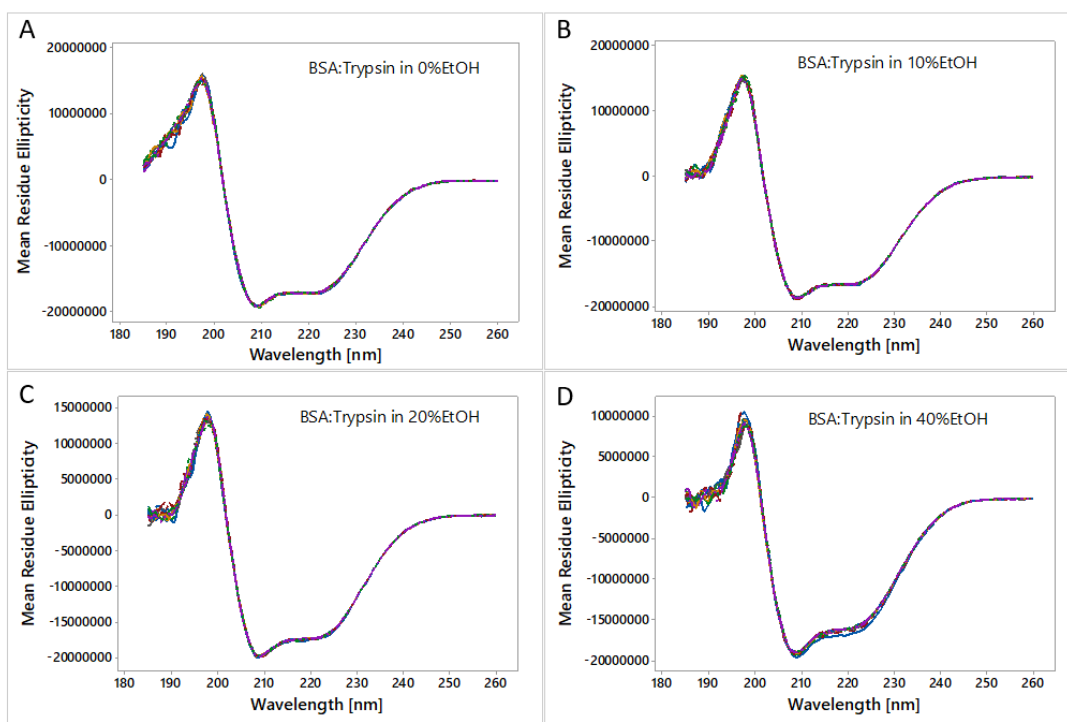


Figure 13. The far-UV CD spectra recorded at 37°C for 90 min of BSA hydrolyzed by trypsin at a ratio of 5000:1 (S:E) in (A) 0% EtOH; (B) 10% EtOH; (C) 20% EtOH; (D) 40% EtOH. (S:0.5 mg/ml and E:0.0001 mg/ml).

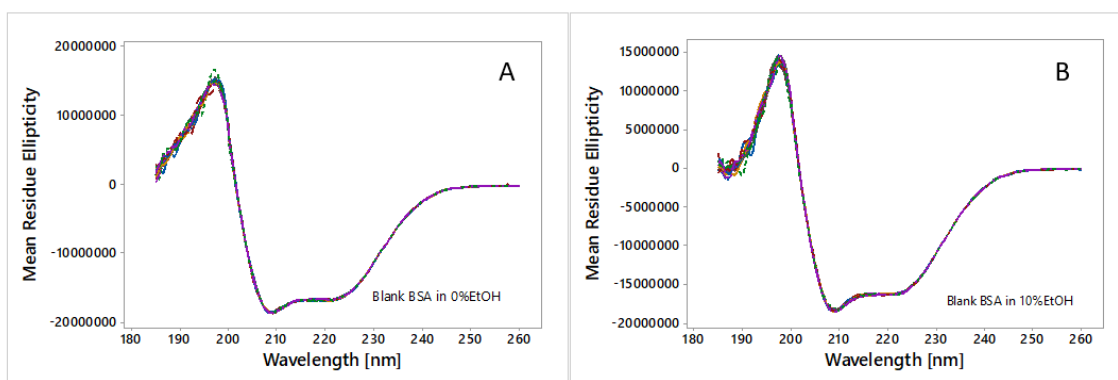


Figure 14. The far-UV CD spectra were recorded at 37°C for 90 min of (A) Blank BSA in pure water buffer (0% EtOH) and (B) Blank BSA in 10% EtOH. (S:0.25 mg/ml).

Figure 13 illustrates the BSA digested by trypsin at the S:E ratio of 5000:1 in 0%, 10%, 20% and 40% EtOH while Figure 14 demonstrates the blank BSA in both pure water buffer and 10% EtOH at 37°C for 90 minutes. The CD spectra of the blank BSA in pure water buffer (0% EtOH) exhibit a typical  $\alpha$ -helical pattern with double

minima at 208 and 222 nm and a maximum around 195 nm which correspond to the characteristics of the  $\alpha$ -helix (Fig. 14A). There is no dramatic change in the intensity for the negative peak at 222 nm for blank BSA when equilibrated in 0% or 10% EtOH in the absence of the trypsin. In the presence of 10% EtOH (Fig. 14B), the far UV-CD spectra profile is similar to that observed in the absence of EtOH (pure water buffer), except for slight intensity changes. It indicates that there is no harsh effect of low EtOH concentrations on the secondary structures of the BSA.

Figure 13 and Figure 15A illustrate that the BSA reacts differently with the varying ethanol concentration in the course of hydrolysis, as indicated by slight alterations in the intensity. Figure 15 demonstrates the mean residue ellipticity at 222 nm for BSA digested by trypsin at a ratio of 5000:1 (S:E) in pure water buffer and also in 10 %, 20%, 40% EtOH, together with blank BSA in both pure water buffer and 10% EtOH at 37°C as a function of time (90 minutes). For Blank BSA (Fig. 15B), there are no important changes in the CD spectra between the conditions of 0% and 10% EtOH. It can be stated that there are no distinct effects of low EtOH concentrations on the secondary structure of the BSA. On the other hand, for hydrolyzed BSA (Fig. 15A), there is a tendency to decrease in the CD signal at 222 nm which means that it becomes less negative upon hydrolysis in all of the ethanol ratios and this indicates that structural components are broken down and BSA is degraded with tryptic hydrolysis. Additionally, it can be seen that high ethanol concentrations (above 20%) cause strong changes in the BSA's secondary structure. The activity of the enzyme is unfavorably affected in the case of high ethanol (40 %EtOH) concentrations. However, when BSA is hydrolyzed in the absence of ethanol, a less negative CD signal is observed at 222 nm, indicating that it causes a more degraded BSA compared to 10% and 20% EtOH.

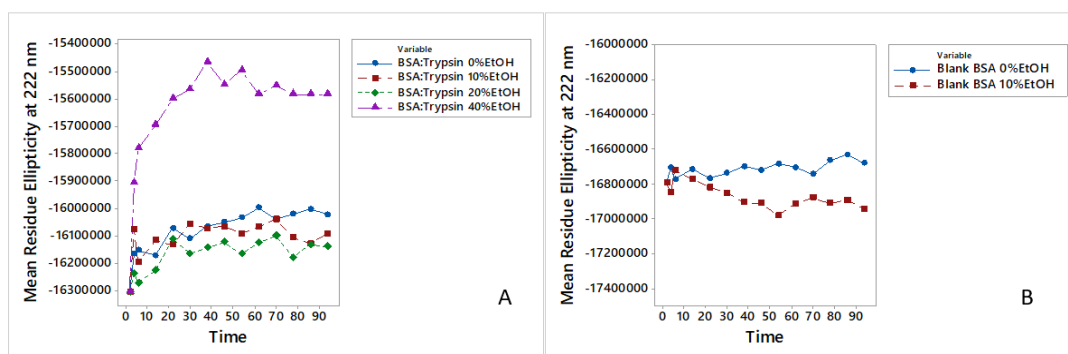


Figure 15. Mean residue ellipticity at 222 nm with respect to time; (A) BSA hydrolyzed by trypsin at a ratio of 5000:1 (S:E) in pure water buffer (0% EtOH) and 10-20-40% EtOH (B) Blank BSA in both 0% EtOH and 10% EtOH at 37°C (plotted from Figs. 13 and 14.). To see the alterations all data points have been initialized in the same point (for the y-axis).

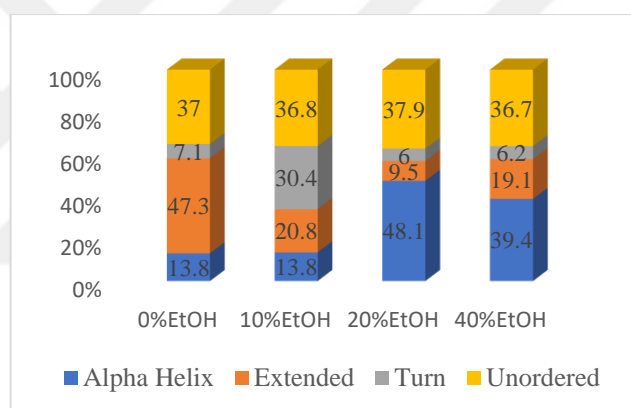


Figure 16. Secondary structure percentages for BSA hydrolyzed by trypsin at the S:E ratio of 5000:1 in 0%, 10%, 20% and 40% EtOH were obtained from the CD spectra at 37°C for t=60 min by using CONTINLL, SELCON3, and CDSSTR methods.

Figure 16 demonstrates the secondary structure analysis of tryptic hydrolysis of BSA at a ratio of 5000:1 (S:E) in 0%, 10%, 20% and 40% EtOH at the end of the 60<sup>th</sup> minute (t=60 min). Analysis was carried out using the CDPro software program which contains CONTINLL, SELCON3 and CDSSTR methods, as explained in (Güler et al., 2016; Güler et al., 2011). As seen in Figure 16, with 0% EtOH, the  $\alpha$ -helix content decreases while extended structures and unordered structures increase at t=60 minutes. For the 10% EtOH condition, a decrease in the  $\alpha$ -helix content, but an increase in the turn and unordered structures at t=60 min due to hydrolysis was

observed. However, the  $\alpha$ -helix content is harshly affected due to the tryptic hydrolysis at higher concentrations of ethanol (20% EtOH and 40% EtOH) compared to 0% EtOH and 10% EtOH. Thus, it can be concluded that high ethanol concentrations (above 20% EtOH) have a different proteolysis mechanism in the BSA protein.

### ***3.2. FTIR Spectroscopy Analysis of $\beta$ -casein Hydrolyzed by Trypsin in Water-Ethanol Medium***

The  $\beta$ -casein to trypsin ratio was 5000:1 (S:E) in samples prepared in pure water buffer and water-ethanol medium. The  $\beta$ -casein concentration was adjusted to 50 mg/ml (Trypsin: 0.01 mg/ml) and was dissolved in 10 mM potassium phosphate buffer both in pure water buffer and water-ethanol mixtures (10% EtOH v/v).

Figure 17 shows the FTIR absorbance and difference spectra of tryptic digestion of  $\beta$ -casein at a ratio of 5000:1 in H<sub>2</sub>O buffer in the absence (0% EtOH) and presence of EtOH (10% EtOH) at 25°C for 180 minutes together with their difference spectrum. In the case of 0% EtOH, the FTIR difference spectra exhibit a strong increase in the intensities around 1646 cm<sup>-1</sup>, 1630 cm<sup>-1</sup>, 1613 cm<sup>-1</sup> and 1590 cm<sup>-1</sup> while the intensities at around 1700 cm<sup>-1</sup> and 1545 cm<sup>-1</sup> decreased dramatically upon tryptic attack during the digestion. The spectral changes are quite different in the presence of EtOH. In the case of 10% EtOH, a slight increment was observed around 1613-1575 cm<sup>-1</sup>.

The altered band positions are summarized below, and the band assignments were provided as follows, based on the literature (Barth, 2000; Fabian and Măntele, 2002; Güler et al., 2011):

↓ 1700 cm<sup>-1</sup>: strongly H-bonded carboxylic acid groups of protonated Asp/Glu residues together with less H-bonded protein secondary structures.

↓ 1675 cm<sup>-1</sup>: turn/loops

↑ 1646 cm<sup>-1</sup>: unordered structures +  $\alpha$ -helices + OH bending

↑ 1630 cm<sup>-1</sup>:  $\beta$ -sheets + Arg and Lys residues

↑ 1613-1580 cm<sup>-1</sup>: NH<sub>2</sub> bending vibrations (proteolysis product)

↑ 1580-1560 cm<sup>-1</sup>:  $\nu_{as}(\text{COO}^-)$  (proteolysis product)

↓ 1545 cm<sup>-1</sup>: unordered structures +  $\alpha$ -helices

↑ 1526 cm<sup>-1</sup>: Lys residues

↑ 1390 cm<sup>-1</sup>:  $\nu_s(\text{COO}^-)$  (proteolysis product)

These altogether strongly indicate that in the absence of EtOH (strong changes) (Fig. 17A, B, and Figs.18,19) and the presence of 10% EtOH (weak changes) (Fig. 17C, D and Figs.18,19); protein secondary structures are altered, turn/loops and regular helical structures decrease while the number of unordered structures and  $\beta$ -sheets increase, the signals of Arg and Lys residues intensify, the amino nitrogen groups and free carboxyl molecular groups are released as proteolysis products during proteolysis of  $\beta$ -casein. An increase in the  $\beta$ -sheet signals is most likely associated with the micelle formation due to a tryptic attack. Accordingly, the peak at  $1646\text{ cm}^{-1}$  might arise also from polyproline II (PPII) structures due to the formations of the micelles. However, the unordered structures, short helices, Arg and Lys residues overlap in the amide I region in the  $\text{H}_2\text{O}$  buffer conditions.

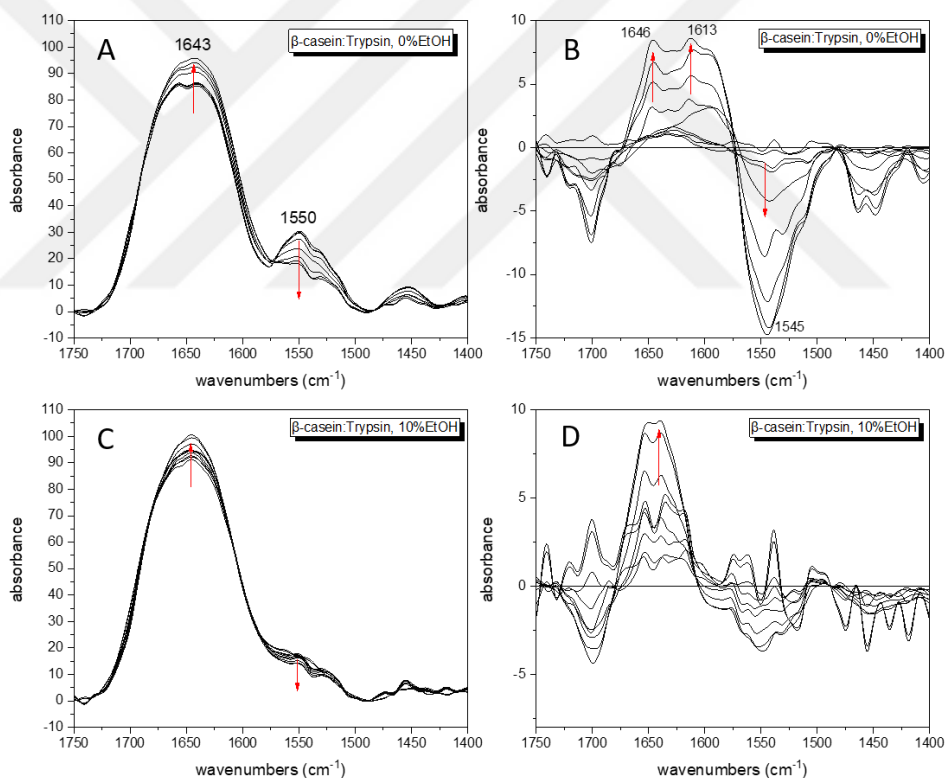


Figure 17. FTIR absorbance spectra of  $\beta$ -casein digested by trypsin at the 5000:1 ratio in (A) 0% EtOH (C) 10% EtOH at  $25^\circ\text{C}$  for 180 minutes. Difference spectra of (B) 0% and (D) 10% EtOH. Difference spectra were acquired from subtraction of the first spectrum taken at  $t_0 = 1\text{ min}$  from each of the absorbance spectra taken during digestion,  $\Delta\text{Absorbance} = \{\text{Digested } \beta\text{-casein (t)}\} - \{\text{Digested } \beta\text{-casein (t}_0 = 1\text{ min)}\}$ . The arrows demonstrate the intensity changes as a function of time.

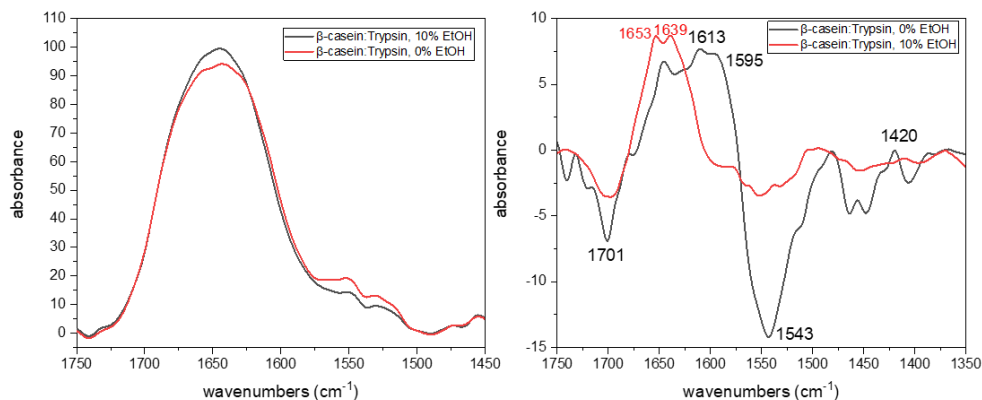


Figure 18. (Left) FTIR absorbance spectra of  $\beta$ -casein digested by trypsin at a 5000:1 ratio in 0% (Red) and 10% (Black) EtOH at 25°C ( $t=120$  min); (Right) Difference spectra of the absorbance spectra of  $\beta$ -casein digested by trypsin at a 5000:1 ratio in 0% (Black) and 10% (Red) EtOH at 25 °C after 2 hours of hydrolysis ( $t=120$  min).

Figure 18 demonstrates the FTIR absorbance spectra of  $\beta$ -casein digested by trypsin at the 5000:1 ratio in 0% EtOH and 10% EtOH together with their difference spectra. The increased signal at around  $1613\text{ cm}^{-1}$  band is striking which is most likely due to liberated  $\text{NH}_2$  groups as the proteolysis products. Additionally, the intensities at  $1420/1390\text{ cm}^{-1}$  and  $1595\text{ cm}^{-1}$  attributed to the symmetric and antisymmetric stretching of free carboxylates, respectively, increase significantly attributed to the proteolysis products (for band assignments see ref (Barth, 2000; Güler et al., 2011)).

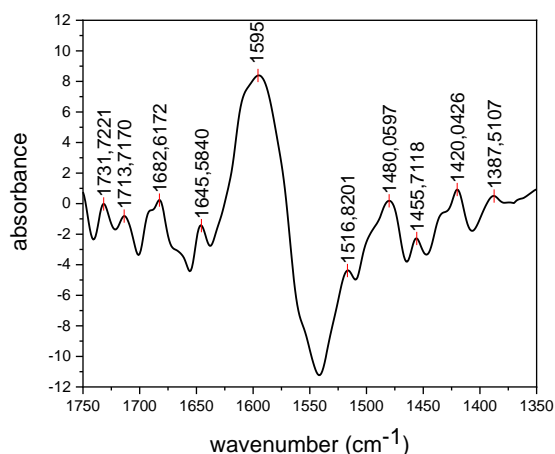


Figure 19. Double difference spectrum of  $\beta$ -casein hydrolyzed by trypsin at a ratio of 5000:1 in 0% EtOH and 10% EtOH. Double difference spectrum was acquired from Figure 18 by subtracting the  $\Delta$ Abs of 10% EtOH from  $\Delta$ Abs of 0% EtOH absorbance spectra,  $\Delta$ Absorbance =  $\{\Delta$ Abs of 0% EtOH (t=120 min) $\} - \{\Delta$ Abs of 10% EtOH (t=120min) $\}$ , at 25 °C.

Figure 19 illustrates the double-difference spectrum of tryptic hydrolysis of  $\beta$ -casein at a ratio of 5000:1 in 0% EtOH and 10% EtOH at t=120 min. After 120 min of proteolysis, the content of  $\alpha$ -helix ( $1656\text{ cm}^{-1}$ ) structures decreases whereas unordered structures ( $1646\text{ cm}^{-1}$ ) increase in the absence of EtOH when compared to 10% EtOH (Fig. 19). In 0% EtOH, a broad positive band between  $1630\text{ cm}^{-1}$  and  $1570\text{ cm}^{-1}$ , attributed mainly to the side chains (such as Arg, Lys) and also  $\beta$ -sheets ( $1630$  and  $1683\text{ cm}^{-1}$ ), also increases. The positive IR signals absorbing at around  $1580\text{ cm}^{-1}$  and  $1420/1390\text{ cm}^{-1}$  bands arise from the  $\text{COO}^-$  vibrations which are the proteolysis products. Furthermore, the IR signals absorbing at around  $1610\text{ cm}^{-1}$  and  $1595\text{ cm}^{-1}$  bands are due to the  $\text{NH}_2$  bending vibrations which can be also regarded as being proteolysis products. In 0% EtOH, we can notice the existence of negative IR signals at around  $1545\text{ cm}^{-1}$  ( $\alpha$ -helix) and  $1672\text{ cm}^{-1}$  (turn), indicating that helices and turns/loops decrease further in 0% EtOH upon digestion when compared to 10% EtOH.

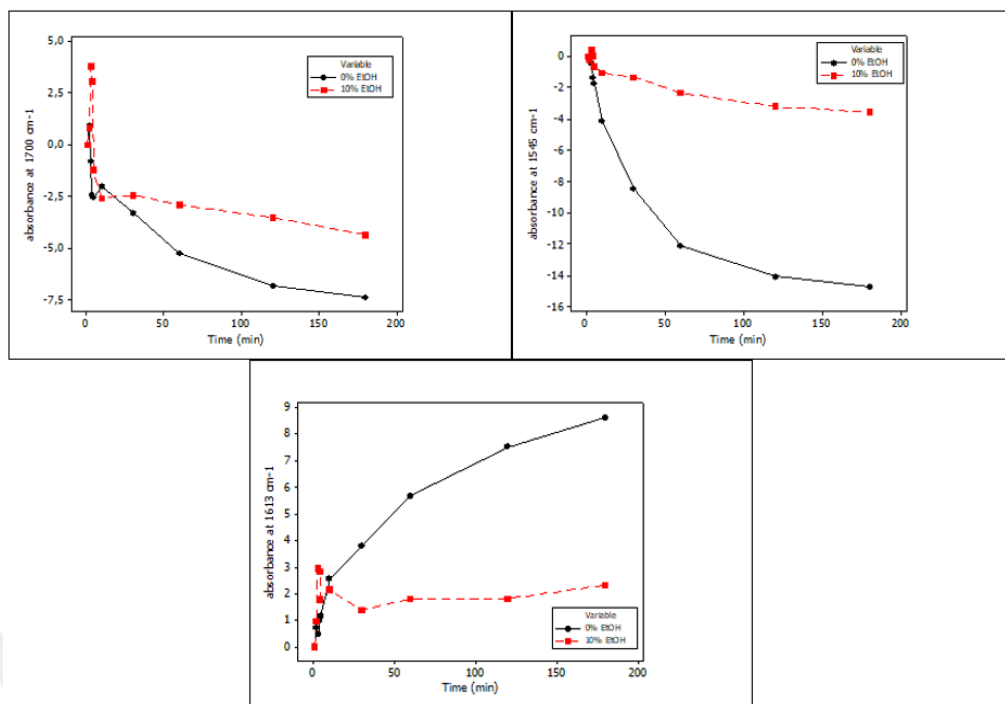


Figure 20. The intensity changes at  $1700\text{ cm}^{-1}$ ,  $1545\text{ cm}^{-1}$ , and at  $1613\text{ cm}^{-1}$  obtained from difference spectra with S:E ratio of 5000:1 ( $\beta$ -casein:Trypsin) in 0% and 10% EtOH at  $25^\circ\text{C}$ . (Red: 10% EtOH; Black: 0% EtOH)

Quantitatively, as can be observed from Figure 20, the intensity at  $1613\text{ cm}^{-1}$  increases largely in 0% EtOH ( $\text{NH}_2$  proteolysis product) whereas the intensities at both  $1700\text{ cm}^{-1}$  and  $1545\text{ cm}^{-1}$  decrease drastically in 0% EtOH at  $25^\circ\text{C}$ . However, such intensity alterations are less dramatic in the presence of 10% EtOH.

### 3.2.1. Two-dimensional correlation spectroscopy (2DCOS) analysis of Tryptic Hydrolysis of $\beta$ -casein in Water-Ethanol Medium

In the synchronous spectra, the peaks are positioned on the diagonal which are always positive and it shows the in-phase cross-correlation between the bands. The synchronous spectra illustrate the intensity changes in the auto peaks (de la Arada et al., 2012). Figure 21 illustrates the 3D plot of FTIR absorbance spectra of tryptic hydrolysis of  $\beta$ -casein at an S:E ratio of 5000:1 in the absence of EtOH. In the synchronous ( $\Phi$ ) 2DCOS map (Fig. 22, Left), the most significant changes are extracted from broad auto peaks in the range of  $1660\text{--}1590\text{ cm}^{-1}$  (maximizing at  $1646$  (unordered) and  $1610\text{ cm}^{-1}$  (NH groups)), at  $1545\text{ cm}^{-1}$  ( $\alpha$ -helices) and also at  $1701$

$\text{cm}^{-1}$  (strongly H-bonded carboxylic acid groups of protonated Asp/Glu residues), positioned in the diagonal that have positive signs. The intensity alterations at 1660-1590  $\text{cm}^{-1}$  and 1545  $\text{cm}^{-1}$  (or 1701  $\text{cm}^{-1}$ ) are in the opposite directions which represents a negative correlation between these auto peaks. This indicates that the intensity of one of these bands increases (1660-1590  $\text{cm}^{-1}$ , as we observed in Fig.21, Fig.17A, B) while the other bands decrease in intensity (1545  $\text{cm}^{-1}$  and 1701  $\text{cm}^{-1}$ ). However, intensity changes at 1545  $\text{cm}^{-1}$  and 1701  $\text{cm}^{-1}$  are in the same direction which represents a positive correlation. This indicates that the intensity of both bands decreases, as detected previously in the absorbance and difference spectra, which was explained above in detail.

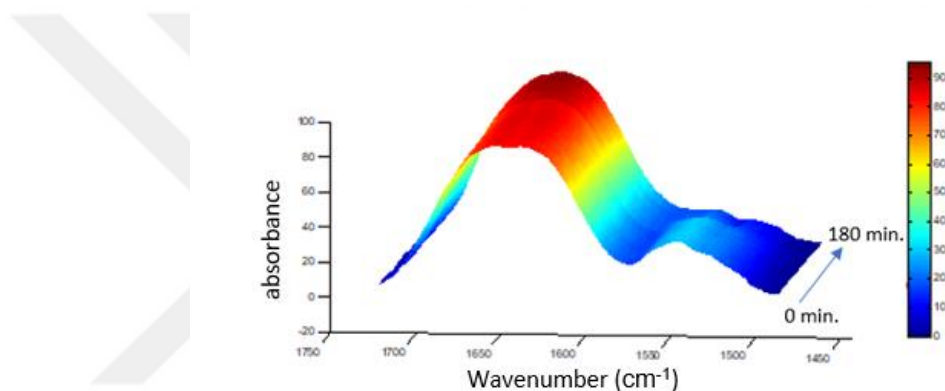


Figure 21. Three-dimensional plot of FTIR absorbance spectrum of  $\beta$ -casein digested by trypsin at a 5000:1 ratio in 0% EtOH at 25°C for 180 minutes.

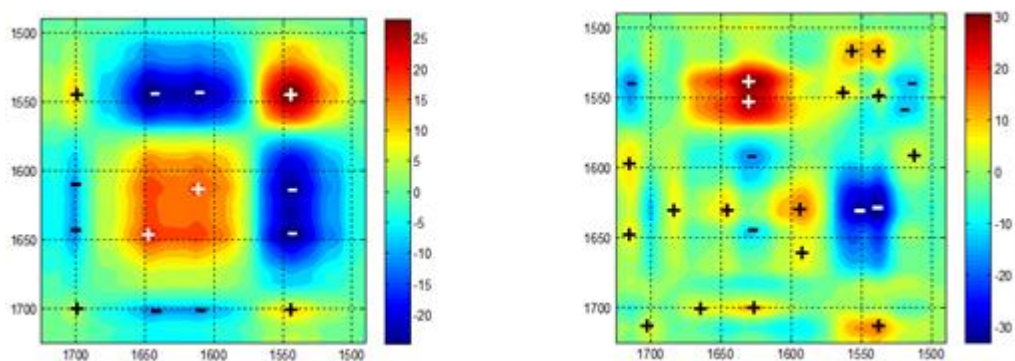


Figure 22. Synchronous (Left) and asynchronous (Right) 2D FTIR correlation spectrum of  $\beta$ -casein digested by trypsin at the S:E ratio of 5000:1 in 0% EtOH at 25°C for 180 minutes.

The information about the sequence of events during proteolysis can be obtained from the asynchronous ( $\Psi$ ) map (Figure 22, Right). Table 4 obtained from Figure 22, demonstrates the correlated band pairs in wavenumber associated with the order of molecular events that take place in the course of proteolysis.

Table 4. Asynchronous correlated peaks of  $\beta$ -casein digested by trypsin (5000:1 ratio) in 0% EtOH at 25°C for 180 min.

Asynchronous correlated peaks (The sign of the peak in the asynchronous map (Sign), the sign of the same area in the synchronous map (Area ( $\Phi$ )), and the order of event are shown)				
Pairs (x/y) ( $\text{cm}^{-1}$ )	Sign	Area ( $\Phi$ ) (Sign of the same area in synchronous map)	Order of event	Order of event with $\text{cm}^{-1}$
1520 / 1540	—	+	←	1540 → 1520
1520 / 1590	+	—	←	1590 → 1520
1520 / 1560	—	+	←	1560 → 1520
1540 / 1710	+	+	→	1540 → 1710
1540 / 1630	—	—	→	1540 → 1630
1540 / 1550	+	+	→	1540 → 1550
1560 / 1630	—	—	→	1560 → 1630
1570 / 1540	+	+	→	1570 → 1540
1590 / 1630	+	+	→	1590 → 1630
1590 / 1660	+	+	→	1590 → 1660
1630 / 1700	+	—	←	1700 → 1630
1630 / 1645	—	+	←	1645 → 1630
1645 / 1700	+	—	←	1700 → 1645
1685 / 1645	+	+	→	1685 → 1645
1660 / 1700	+	—	←	1700 → 1660
1685 / 1630	+	+	→	1685 → 1630
1701 / 1710	+	+	→	1701 → 1710

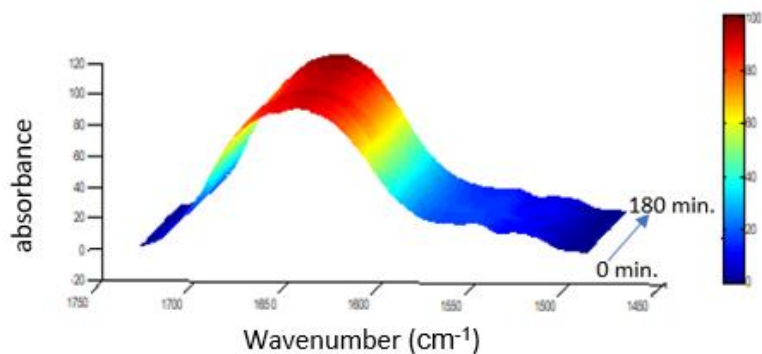


Figure 23. A 3D plot of IR absorbance spectra of  $\beta$ -casein digested by trypsin (5000:1) in 10% EtOH at 25°C for 180 min.

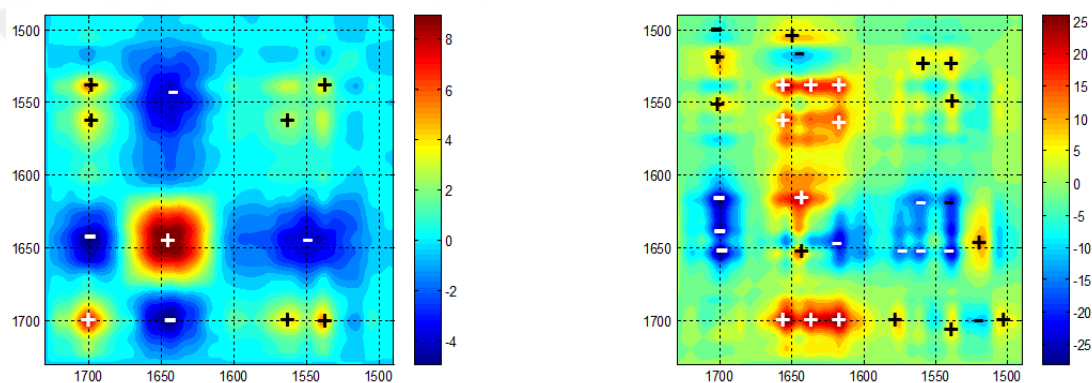


Figure 24. Synchronous (Left) and asynchronous (Right) 2D FTIR correlation spectra of  $\beta$ -casein digested by trypsin at the 5000:1 ratio in 10% EtOH at 25°C for 180 minutes.

Figure 23 demonstrates the 3D plot of FTIR absorbance spectra of tryptic hydrolysis of  $\beta$ -casein in 10% EtOH. In the synchronous ( $\Phi$ ) 2DCOS map, the most important changes are extracted from broad auto peaks at 1648 (unordered), 1570  $\text{cm}^{-1}$  (NH groups), 1540  $\text{cm}^{-1}$  ( $\alpha$ -helices) and also at 1700  $\text{cm}^{-1}$  (strongly H-bonded carboxylic acid groups of protonated Asp/Glu residues), positioned in the diagonal that have positive signs (Fig. 24, Left). The intensity alterations at 1648  $\text{cm}^{-1}$  and 1540/1570/1700  $\text{cm}^{-1}$  are in the opposite directions, representing a negative correlation between these auto peaks. This indicates that the intensity of one of these bands increases (1648  $\text{cm}^{-1}$ , as we have observed formerly in Fig.23 and Fig.16C, D) while the other bands decrease in intensity (1540  $\text{cm}^{-1}$ , 1570  $\text{cm}^{-1}$  and 1700  $\text{cm}^{-1}$ ). However, intensity changes at 1540  $\text{cm}^{-1}$ , 1570  $\text{cm}^{-1}$  and 1700  $\text{cm}^{-1}$  are in the same directions,

representing a positive correlation which indicates that the intensities of those bands decrease, as we have detected previously in the absorbance and difference spectra.

The information regarding the order of events was obtained from the asynchronous ( $\Psi$ ) map (Fig. 24, Right). Table 5 obtained from Figure 24 demonstrates the correlated FTIR band pairs associated with the sequence of molecular events that occur as the proteolysis proceeds.

Table 5. Asynchronous correlated peaks of  $\beta$ -casein digested by trypsin (5000:1) in 10% EtOH at 25°C for 180 minutes.

Asynchronous correlated peaks (The sign of the peak in the asynchronous map (Sign), the sign of the same area in the synchronous map (Area ( $\Phi$ )), and the order of event are shown)				
Pairs (x/y) ( $\text{cm}^{-1}$ )	Sign	Area ( $\Phi$ ) (Sign of the same area in synchronous map)	Order of event	Order of event with $\text{cm}^{-1}$
1520 / 1700	—	+	→	1700 → 1520
1520 / 1645	+	—	←	1645 → 1520
1540 / 1700	+	+	→	1540 → 1700
1540 / 1655	—	—	→	1540 → 1655
1540 / 1632	—	—	→	1540 → 1632
1540 / 1520	—	—	→	1540 → 1520
1560 / 1632	—	—	→	1560 → 1632
1560 / 1620	—	—	→	1560 → 1620
1572 / 1700	+	+	→	1572 → 1700
1590 / 1660	+	+	→	1590 → 1660
1632 / 1700	+	—	←	1700 → 1632
1632 / 1620	+	+	→	1632 → 1620
1632 / 1520	—	—	→	1632 → 1520
1655 / 1700	+	—	←	1700 → 1655
1655 / 1645	—	+	←	1645 → 1655

Table 5 (cont'd)

1655 / 1620	+	+	→	1655 → 1620
1655 / 1560	+	—	←	1560 → 1655
1645 / 1700	+	—	←	1700 → 1645
1655 / 1572	+	—	←	1572 → 1655

Even though the correlated peaks are not the same for both EtOH concentrations (Table 4, 5), as can be seen from the peak signs, the sequence of molecular events that are observed during the time course of proteolysis are very similar for both the EtOH concentrations (0% and 10%), as follows:

**5000:1, 0% EtOH:**

1570 cm<sup>-1</sup> → 1540 cm<sup>-1</sup>/1560 cm<sup>-1</sup>/1590 cm<sup>-1</sup>/1700 cm<sup>-1</sup>/1685 cm<sup>-1</sup> → 1645 cm<sup>-1</sup> → 1660 cm<sup>-1</sup>/1630 cm<sup>-1</sup>/1550 cm<sup>-1</sup>/1710 cm<sup>-1</sup>/1520 cm<sup>-1</sup>

**5000:1, 10% EtOH:**

1572 cm<sup>-1</sup>/1540 cm<sup>-1</sup>/1560 cm<sup>-1</sup> → 1700 cm<sup>-1</sup> → 1645 cm<sup>-1</sup> → 1655 cm<sup>-1</sup>/1632 cm<sup>-1</sup> → 1620 cm<sup>-1</sup>/1520 cm<sup>-1</sup>

These spectral signatures can be converted into the order of events. In 0% EtOH, the first change occurs at 1570 cm<sup>-1</sup> (COO<sup>-</sup> of Glu/Asp). Then, the IR bands related to proteolysis products (NH<sub>2</sub> and COO<sup>-</sup>), strongly H-bonded Asp/Glu residues, turn/loops, and helical structures start to change (1590 cm<sup>-1</sup>, 1560 cm<sup>-1</sup>, 1700 cm<sup>-1</sup>, 1685 cm<sup>-1</sup>, 1540 cm<sup>-1</sup>, respect.). After that, the IR band at 1645 cm<sup>-1</sup> (unordered structures/OH bending) starts to change for both of the EtOH concentrations. Then, the IR bands absorbing at 1660 cm<sup>-1</sup> ( $\alpha$ -helix/unordered), 1630 cm<sup>-1</sup> ( $\beta$ -sheets/Arg/Lys), 1550 cm<sup>-1</sup> ( $\alpha$ -helix), 1710 cm<sup>-1</sup> (relatively weak H-bonded Glu/Asp residues) and at 1520 cm<sup>-1</sup> (Lys) starts to change in 0% EtOH.

In 10% EtOH, the first change occurs at 1572 cm<sup>-1</sup>, 1560 cm<sup>-1</sup> and 1540 cm<sup>-1</sup> with a decrease in the Asp/Glu and  $\alpha$ -helical signals. The statement of decrease/increase was interpreted based on the difference spectrum while the changes were interpreted from the asynchronous map. Then, the signal at 1700 cm<sup>-1</sup> (strongly H-bonded Asp/Glu) decreases. Afterward, the IR band at 1645 cm<sup>-1</sup> (unordered structures / OH bending) starts to change. This is followed by intensity alterations at

1655  $\text{cm}^{-1}$  ( $\alpha$ -helices) and 1632  $\text{cm}^{-1}$  (attributed to  $\beta$ -sheets/Arg/Lys) which increase in the presence of 10% EtOH. Finally, the intensities at 1620  $\text{cm}^{-1}$  and 1520  $\text{cm}^{-1}$  change (increase), tentatively attributed to the  $\text{NH}_2$  groups (and/or Lys).

### 3.2.2. Secondary Structure Analysis of Tryptic Hydrolysis of $\beta$ -casein in Water-Ethanol Medium

The secondary structure analysis was carried out by using the curve-fitting procedure. Figure 25 illustrates the curve fit analysis for the amide I region at  $t=1$  min and  $t=120$  min of  $\beta$ -casein digested by trypsin in the absence of ethanol (5000:1 in 0% EtOH) in  $\text{H}_2\text{O}$  buffer at  $25^\circ\text{C}$ , and the quantitative results are shown in Table 6.

As shown in detail in Table 6, the secondary structure content of  $\beta$ -casein digested by trypsin in the absence of ethanol (5000:1 in 0% EtOH) in  $\text{H}_2\text{O}$  buffer at  $25^\circ\text{C}$  is composed of 23.7%  $\beta$ -sheets, 28.6% turn/loops and 47.7%  $\alpha$ -helix/short helices/random coil structures at  $t=1$  min. However, at  $t=120$  min, digested  $\beta$ -casein is composed of 32.4%  $\beta$ -sheets, 19.3% turn/loops and 48.2%  $\alpha$ -helix/short helices/random coil structures. This indicates that the content of  $\beta$ -sheets increases while the amount of turn/loops decreases as the proteolysis proceeds (at  $t=120$  min). The conformation of helicoid structures and random coils are rearranged in the course of digestion (S:E is 5000:1 in 0% EtOH).

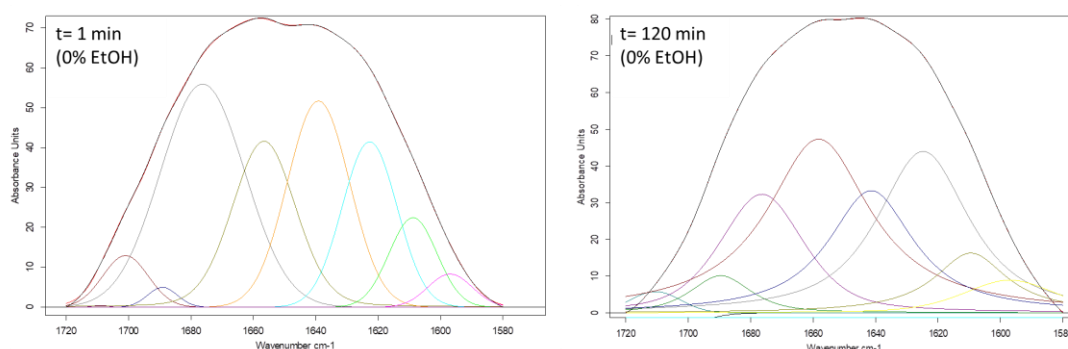


Figure 25. Curve fit analysis of amide I at  $t=1$  min (Left) and  $t=120$  min (Right) of tryptic hydrolysis of  $\beta$ -casein in the absence of ethanol (5000:1 in 0% EtOH) in  $\text{H}_2\text{O}$  buffer at  $25^\circ\text{C}$ . The envelope bands which are formed by curve fitting are shown in red and the env envelope bands of the original spectra are shown in black color. Before the curve fitting, the corresponding enzyme was subtracted from the hydrolyzed  $\beta$ -casein.

Table 6. Assignment of amide I components and percentages (%) of secondary structure elements of  $\beta$ -casein hydrolyzed by trypsin in the absence of ethanol (5000:1 in 0% EtOH) in H<sub>2</sub>O buffer at 25°C (Spectra at t=1 min and t=120 min).

Position in H <sub>2</sub> O (cm <sup>-1</sup> )	Band Assignments <sup>c</sup>	% t=1 min	% t=120 min
1623 <sup>a</sup> , 1689	$\beta$ -sheets	23.7	32.4
1639 <sup>a</sup>	Random coils	26.4	19.9
1657	$\alpha$ -helix/Short helices/ Random coils	21.3	28.3
1676 <sup>b</sup>	Turn/loop	28.6	19.3
<sup>a</sup> Contains elements of amide side chains (Arg, Lys). <sup>b</sup> Contains elements of amide side chains (Arg, Asn, Gln). <sup>c</sup> Band assignments are based on the literature (Barth, 2007; Fabian and Mäntele, 2002; Güler et al., 2011)			

The curve fit analysis was also performed for the amide I region at t=1 min and t=120 min of  $\beta$ -casein digested by trypsin in the presence of ethanol (5000:1 in 10% EtOH) in H<sub>2</sub>O buffer at 25°C, and the estimated percentages of protein secondary structures are given in Table 7. Based on Table 7, the secondary structure content of  $\beta$ -casein digested by trypsin in the presence of ethanol (5000:1 in 10% EtOH) is composed of 39.2%  $\beta$ -sheets, 11.5% turn/loops and 49.3%  $\alpha$ -helix/short helices/random coil structures at t=1 min. However, at t=120 min, digested  $\beta$ -casein is composed of 34.6%  $\beta$ -sheets, 14% turn/loops and 51.3%  $\alpha$ -helix/short helices/random coil structures.

This indicates that in the presence of 10% EtOH the content of  $\beta$ -sheets increases while the amount of turn/loops decrease already at the beginning of digestion (at t=1 min) and less dramatic alterations are observed as the proteolysis proceeds, as also quantitatively seen in Figure 20 above. The conformation and amount of helical structures and random coils are also rearranged in the course of digestion (S:E is 5000:1 in 10% EtOH).

Table 7. Assignment of amide I components and percentages (%) of secondary structures of  $\beta$ -casein digested by trypsin in the presence of 10% Ethanol (5000:1 in 10% EtOH) in H<sub>2</sub>O buffer at 25°C (Spectra at t=1 min and t=120 min).

Position in H <sub>2</sub> O (cm <sup>-1</sup> )	Band Assignments <sup>c</sup>	% t=1 min	% t=120 min
1623 <sup>a</sup> , 1629 <sup>a</sup> , 1684, 1691	$\beta$ sheets / intermolecular $\beta$ - sheets	39.2	34.6
1641 <sup>a</sup> , 1646	Random coils	21.6	26.7
1659, 1666	$\alpha$ -helix/Short helices/Random coils	27.7	24.6
1678 <sup>b</sup>	Turn/loop	11.5	14
<sup>a</sup> Contains elements of amide side chains (Arg, Lys). <sup>b</sup> Contains elements of amide side chains (Arg, Asn, Gln). <sup>c</sup> Band assignments is based on the literature (Barth, 2007; Fabian and Mäntele, 2002; Güler et al., 2011).			

### 3.3. FTIR Spectroscopy Analysis of $\beta$ -casein Hydrolyzed by Trypsin in Deuterium Oxide Buffer

The  $\beta$ -casein to trypsin ratio of the samples prepared in 20 mM potassium phosphate buffer (in deuterium oxide) was 500:1, 4000:1 and 10000:1 (w/w). According to the FTIR-difference spectra for all of the  $\beta$ -casein to trypsin ratios investigated here (Fig. 26), protein secondary structures (for instance  $\beta$ -sheets at 1633 cm<sup>-1</sup> and  $\alpha$ -helices at 1650 cm<sup>-1</sup>) undergo important amide changes, their intensities decrease while intensities at 1593 cm<sup>-1</sup> and 1405 cm<sup>-1</sup> increase as the enzymatic reaction continues for 90 minutes. When the trypsin concentration was too low at S:E=10000, the spectrum alterations were noticed to a lesser extent.

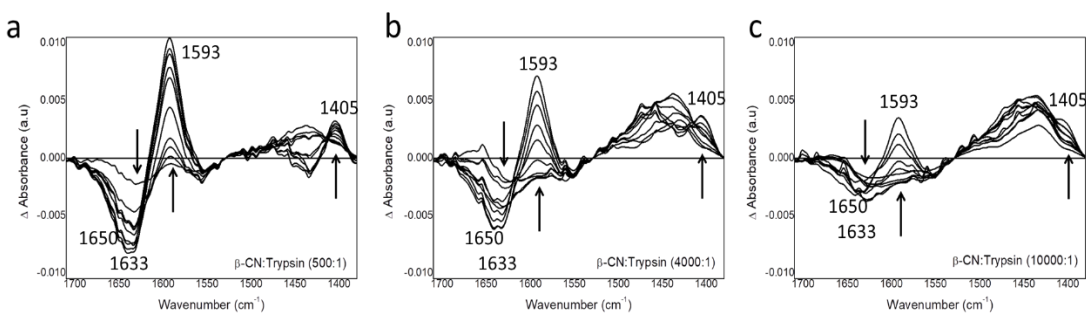


Figure 26. The FTIR difference spectra for  $\beta$ -casein digested by trypsin recorded at  $37^\circ\text{C}$  for the S:E ratios of (a) 500:1, (b) 4000:1 and (c) 10000:1 (w/w). The arrows demonstrate the amide changes of  $\beta$ -casein during digestion as a function of time.

Figure 27 illustrates the changes of intensity at  $1633\text{ cm}^{-1}$  ( $\beta$ -sheet signal),  $1650\text{ cm}^{-1}$  ( $\alpha$ -helix signal) and  $1593\text{ cm}^{-1}$  (antisymmetric stretching of  $\text{COO}^-$  as proteolysis products). Time-dependent graphs were derived from FTIR-difference spectra (Fig. 27) for proteolytic processes performed at the S:E ratios of 500:1, 4000:1, and 10000:1. The fundamental trend is that as the enzymatic activity progresses, the relative content of  $\beta$ -sheet and  $\alpha$ -helical structures declines while the number of free carboxylate groups as proteolysis products increases. At S:E=500:1, a greater amount of enzyme causes more changes, resulting in a greater reduction in the content of both  $\beta$ -sheets and  $\alpha$ -helices of  $\beta$ -casein (Fig. 27a,b) and a greater rise in the content of free carboxylate groups released as a result of the hydrolysis of particular peptide bonds by trypsin (Fig. 27c).

The variations in the content of  $\beta$ -sheets and  $\alpha$ -helical structures during the proteolysis reaction are more complicated at lower enzyme concentrations (S:E=10000:1) (Fig. 27, blue line). The  $\beta$ -sheet content, for example, reduces faster in the early stages of hydrolysis (within the first 5 minutes), but then it increases followed by a decrease again, forming a local maximum. Only 10 minutes after the start of the proteolysis reaction, the proteolysis products ( $1593\text{ cm}^{-1}$ ) start to increase. This clearly shows that the peptide nanoparticles of  $\beta$ -casein are reorganized following the start of proteolysis and that hydrolysis products are released after a lag phase. Similar regularities in the content of  $\beta$ -sheets and  $\alpha$ -helices are found during proteolysis for S:E=4000:1, although the decrease in the content of secondary structures is higher and faster (first 4 minutes) compared to the S:E=10000:1 condition.

The intensity changes detected at  $1593\text{ cm}^{-1}$  (antisymmetric stretching of free carboxylates as proteolysis products),  $1650\text{ cm}^{-1}$  ( $\alpha$ -helix), and  $1633\text{ cm}^{-1}$  ( $\beta$ -sheet) obtained from the FTIR-difference spectra were plotted as a function of time in the course of enzymatic reaction for the  $S_0/E_0$  ratios of 500, 4000 and 10000.

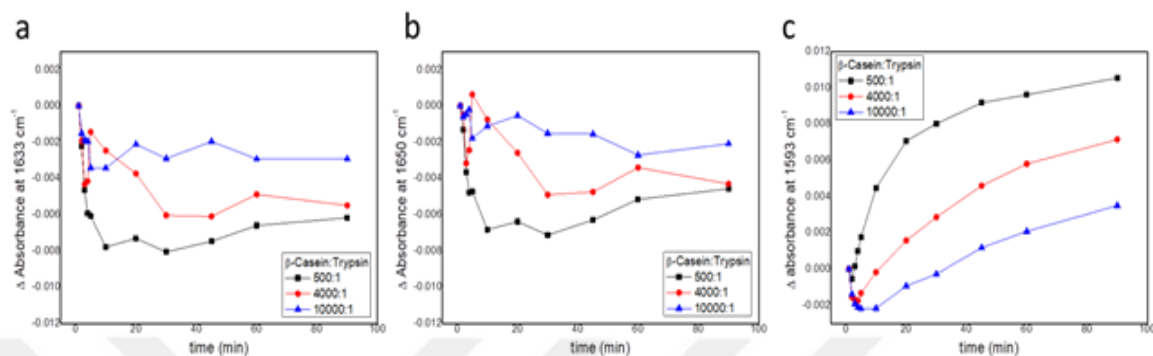


Figure 27. The intensity changes acquired from the FTIR-difference spectra (from Fig. 26) with the S:E ratios of 500:1, 4000:1 and 10000:1 (w/w) as a function of time. The content of (a)  $\beta$ -sheets absorbing at  $1633\text{ cm}^{-1}$ , (b)  $\alpha$ -helix absorbing at  $1650\text{ cm}^{-1}$  and (c) antisymmetric stretching of free carboxylates (products of proteolysis) absorbing at  $1593\text{ cm}^{-1}$ .

## CHAPTER 4: CONCLUSION

Proteolysis can be defined as a natural process where the proteins are enzymatically digested. In this present study, FTIR and CD spectroscopic techniques were used to track and monitor the conformational changes caused by trypsin in the secondary structure of the proteins. The overall goal of this thesis was to demonstrate the suitability and applicability of both spectroscopic techniques for real-time monitoring of the proteolysis mechanism by tracking the spectral changes in tandem with secondary structure analysis.

FTIR spectroscopy enabled the determination of alterations in the secondary structure of  $\beta$ -casein throughout the particle rearrangement, which is crucial information for grasping the proteolysis process at the molecular level. Analysis of FTIR-difference spectra was used to determine the alterations in the contents of  $\beta$ -sheets,  $\alpha$ -helices, and proteolysis products as a function of hydrolysis time. It was shown that, in water-ethanol mixtures, the addition of ethanol changes the proteolysis mechanism from the condition where the masking to demasking transition is predominant to the case where the contribution of unhydrolyzed bonds becomes significant. The effect of ethanol in low concentrations is related to a decrease in intermolecular interactions of the  $\beta$ -casein and also an increase in  $\beta$ -casein's hydration when the addition of ethanol increases the H-bonding of water. The FTIR spectroscopy findings and data analysis revealed that in the absence of EtOH (strong changes) and 10% EtOH (weak changes), protein secondary structures are changed, turn/loops and regular helical structures decrease while the number of unordered structures and  $\beta$ -sheets increases. Furthermore, amino nitrogen groups and free carboxyl molecular groups are released which are the proteolysis products throughout the proteolysis of  $\beta$ -casein.

Additionally, the analysis of the tryptic hydrolysis of  $\beta$ -casein with various concentrations of S:E in deuterium oxide buffer indicated that protein secondary structures undergo crucial amide changes. The free carboxylate groups which are the products of proteolysis released through enzymatic hydrolysis of the intact protein observed via the FTIR spectroscopic method which resulted in a definite indicator for the processes of the proteolysis.

Hydrolysis of BSA by trypsin at 37°C in both pure water buffer and with the addition of EtOH (10, 20 and 40% EtOH v/v) was performed by CD spectroscopy. According to the CD spectroscopy analysis, there is no drastic effect of low ethanol concentrations on the secondary structure of the protein however it was found that with the increasing ethanol concentration BSA's structural components are broken and degraded during the hydrolysis process.

In conclusion, the monitoring of crucial structural and conformational alterations in the secondary structures of proteins is monitored in real-time throughout the enzymatic digestion via CD and FTIR spectroscopic techniques. The data obtained from the spectroscopic methods demonstrates that the secondary structures' of BSA and  $\beta$ -casein loose during proteolysis.



## REFERENCES

- Atamer, Z., Post, A.E., Schubert, T., Holder, A., Boom, R.M. and Hinrichs, J. (2017) *Bovine  $\beta$ -casein: Isolation, properties and functionality. A review*, International Dairy Journal, Elsevier, Vol. 66, pp. 115–125.
- Baker, M.J., Trevisan, J., Bassan, P., Bhargava, R., Butler, H.J., Dorling, K.M., Fielden, P.R., *et al.* (2014) *Using Fourier transform IR spectroscopy to analyze biological materials*, Nature Protocols, Nat Protoc, Vol. 9, No. 8, pp. 1771–1791.
- Bar-Zeev, M., Assaraf, Y.G. and Livney, Y.D. (2016)  *$\beta$ -casein nanovehicles for oral delivery of chemotherapeutic Drug combinations overcoming P-glycoprotein-mediated multidrug resistance in human gastric cancer cells*, Oncotarget, Vol. 7, No. 17, pp. 23322–23334.
- Barth, A. (2000) *The infrared absorption of amino acid side chains*, Progress in Biophysics and Molecular Biology, Vol. 74, No. 3–5, pp. 141–173.
- Barth, A. (2007) *Infrared spectroscopy of proteins*, Biochimica et Biophysica Acta - Bioenergetics, Vol. 1767, No. 9, pp. 1073–1101.
- Barth, A. and Zscherp, C. (2002) *What vibrations tell us about proteins*, Quarterly Reviews of Biophysics, Q Rev Biophys, Vol. 35, No. 4, pp. 369–430.
- Berg, J.M., Tymoczko, J.L. and Stryer, L. (2002) *Biochemistry*, edited by Berg, J.M., Tymoczko, J.L. and Stryer, L. Biochemistry, 5th edition, 4. print., W.H. Freeman Publishing, New York NY.
- Carter, D.C. and Ho, J.X. (1994) *Structure of Serum Albumin*, Advances in Protein Chemistry, Academic Press, Vol. 45, No. C, pp. 153–203.
- Corrêal, D. and Ramos, C.H.I.R. (2009) *The use of circular dichroism spectroscopy to study protein folding, form and function*, African J Biochem Res, Academic Journals, Vol. 3, No. 5, pp. 164–173.
- Dufour, E. and Haertl', T. (1990) *Alcohol-induced changes of  $\beta$ -lactoglobulin - retinol-binding stoichiometry*, Protein Engineering, Design and Selection, Oxford Academic, Vol. 4, No. 2, pp. 185–190.
- Erez, E., Fass, D. and Bibi, E. (2009) *How intramembrane proteases bury hydrolytic reactions in the membrane*, Nature 2009 459:7245, Nature Publishing Group, Vol. 459, No. 7245, pp. 371–378.
- Fabian, H. and Mäntele, W. (2002) *Infrared Spectroscopy of Proteins*, Handbook of Vibrational Spectroscopy, John Wiley & Sons, Chichester, UK, pp. 3399–3425.

- Farrell, H.M., Jimenez-Flores, R., Bleck, G.T., Brown, E.M., Butler, J.E., Creamer, L.K., Hicks, C.L., *et al.* (2004) *Nomenclature of the proteins of cows' milk - Sixth revision*, Journal of Dairy Science, Elsevier, Vol. 87, No. 6, pp. 1641–1674.
- Finlayson, D., Rinaldi, C. and Baker, M.J. (2019) *Is Infrared Spectroscopy Ready for the Clinic?*, Analytical Chemistry, Vol. 91, No. 19, pp. 12117–12128.
- Forrest, S.A., Yada, R.Y. and Rousseau, D. (2005) *Interactions of vitamin D3 with bovine  $\beta$ -lactoglobulin A and  $\beta$ -casein*, Journal of Agricultural and Food Chemistry, J Agric Food Chem, Vol. 53, No. 20, pp. 8003–8009.
- Głąb, T.K. and Boratyński, J. (2017) *Potential of Casein as a Carrier for Biologically Active Agents*, Topics in Current Chemistry (Cham), Vol. 375, No. 4.
- Grosclaude, F., Mahé, M. -F and Ribadeau-Dumas, B. (1973) *Structure primaire de la caséine  $\alpha$ 1 et de la caséine  $\beta$  bovines: Correctif*, European Journal of Biochemistry, Vol. 40, No. 1, pp. 323–324.
- Güler, G., Džafić, E., Vorob'ev, M.M., Vogel, V. and Mäntele, W. (2011) *Real time observation of proteolysis with Fourier transform infrared (FT-IR) and UV-circular dichroism spectroscopy: watching a protease eat a protein*, Spectrochimica Acta. Part A, Molecular and Biomolecular Spectroscopy, Vol. 79, pp. 104–111.
- Güler, G., Vorob'ev, M.M., Vogel, V. and Mäntele, W. (2016) *Proteolytically-induced changes of secondary structural protein conformation of bovine serum albumin monitored by Fourier transform infrared (FT-IR) and UV-circular dichroism spectroscopy*, Spectrochimica Acta. Part A, Molecular and Biomolecular Spectroscopy, Vol. 161, pp. 8–18.
- Hirayama, K., Akashi, S., Furuya, M. and Fukuhara, K. ichi. (1990) *Rapid confirmation and revision of the primary structure of bovine serum albumin by ESIMS and frit-FAB LC/MS*, Biochemical and Biophysical Research Communications, Academic Press, Vol. 173, No. 2, pp. 639–646.
- Hoffmann, S.V., Fano, M. and van de Weert, M. (2016) *Circular Dichroism Spectroscopy for Structural Characterization of Proteins*, New York, NY : Springer, pp. 223–251.
- Holt, C. (1992) *Structure and Stability of Bovine Casein Micelles*, Advances in Protein Chemistry, Vol. 43, pp. 63–151.
- Holzwarth, G. and Doty, P. (1965) *THE ULTRAVIOLET CIRCULAR DICHROISM OF POLYPEPTIDES*, Journal of the American Chemical Society, J Am Chem Soc, Vol. 87, No. 2, pp. 218–228.

- Konnova, T.A., Faizullin, D.A., Haertle, T. and Zuev, Y.F. (2013)  *$\beta$  Casein Micelle Formation in Water – Ethanol Solutions*, Vol. 448, No. 4, pp. 480–483.
- Kundu, S., Aswal, V.K. and Kohlbrecher, J. (2017) *Effect of ethanol on structures and interactions among globular proteins*, Chemical Physics Letters, Elsevier B.V., Vol. 670, pp. 71–76.
- de la Arada, I., Seiler, C. and Mäntele, W. (2012) *Amyloid fibril formation from human and bovine serum albumin followed by quasi-simultaneous Fourier-transform infrared (FT-IR) spectroscopy and static light scattering (SLS)*, European Biophysics Journal: EBJ, Vol. 41, No. 11, pp. 931–8.
- Langbein, W. and Borri, P. (2014) *Resonant Nonlinear Optical Microscopy*, Proceedings of the International School of Physics “Enrico Fermi”, IOS Press, Vol. 181, pp. 141–173.
- Liu, R., Qin, P., Wang, L., Zhao, X., Liu, Y. and Hao, X. (2010) *Toxic Effects of Ethanol on Bovine Serum Albumin*, Vol. 24, No. 1, pp. 66–71.
- Lu, R., Li, W.W., Katzir, A., Raichlin, Y., Yu, H.Q. and Mizaikoff, B. (2015) *Probing the secondary structure of bovine serum albumin during heat-induced denaturation using mid-infrared fiberoptic sensors*, Analyst, Royal Society of Chemistry, Vol. 140, No. 3, pp. 765–770.
- Manea, M., Mezo, G., Hudecz, F. and Przybylski, M. (2007) *Mass spectrometric identification of the trypsin cleavage pathway in lysyl-proline containing oligopeptides*, Journal of Peptide Science: An Official Publication of the European Peptide Society, J Pept Sci, Vol. 13, No. 4, pp. 227–236.
- Martin, S.R. and Schilstra, M.J. (2008) *Circular Dichroism and Its Application to the Study of Biomolecules*, Methods in Cell Biology, Academic Press, Vol. 84, pp. 263–293.
- Noda, I. (2007) *Two-dimensional correlation analysis useful for spectroscopy, chromatography, and other analytical measurements*, Analytical Sciences: the international journal of the Japan Society for Analytical Chemistry, Vol. 23, pp. 139–146.
- Noda, I. and Ozaki, Y. (2005) *Two-Dimensional Correlation Spectroscopy: Applications in Vibrational and Optical Spectroscopy*. 1st edition. John Wiley & Sons.
- Owen, C.A. (2006) *SERINE PROTEINASES*, Encyclopedia of Respiratory Medicine, Four-Volume Set, Academic Press, pp. 1–10.
- Polgár, L. (2005) *The catalytic triad of serine peptidases*, Cellular and Molecular Life

- Sciences, Vol. 62, No. 19–20, pp. 2161–2172.
- Rodger, A. (2018) *Far UV protein circular dichroism*, Encyclopedia of Biophysics, Springer, Springer Nature, pp. 1–6.
- Sreerama, N. and Woody, R.W. (2000) *Estimation of Protein Secondary Structure from Circular Dichroism Spectra: Comparison of CONTIN, SELCON, and CDSSTR Methods with an Expanded Reference Set*, Vol. 260, pp. 252–260.
- Stryer, L. (1988) *Book Reviews Biochemistry (Third Edition) Electrophoresis. Theory, Techniques, and Biochemical and Clinical Applications (Second Edition)*, Biochemistry, Vol. 16, No. 3, pp. 181–182.
- Subramanian, A. and Rodriguez-Saona, L. (2009) *Fourier Transform Infrared (FTIR) Spectroscopy*, Infrared Spectroscopy for Food Quality Analysis and Control, Academic Press, pp. 145–178.
- Tavano, O.L., Berenguer-Murcia, A., Secundo, F. and Fernandez-Lafuente, R. (2018) *Biotechnological Applications of Proteases in Food Technology*, Comprehensive Reviews in Food Science and Food Safety, John Wiley & Sons, Ltd, Vol. 17, No. 2, pp. 412–436.
- Tchorbanov, B. and Iliev, I. (1993) *Limited enzymic hydrolysis of casein in the presence of ethanol*, Enzyme and Microbial Technology, Elsevier, Vol. 15, No. 11, pp. 974–978.
- Vorob'ev, M.M., Strauss, K., Vogel, V. and Mäntele, W. (2015) *Demasking of Peptide Bonds During Tryptic Hydrolysis of  $\beta$ -casein in the Presence of Ethanol*, Food Biophysics, Vol. 10, No. 3, pp. 309–315.
- Walstra, P. (1990) *On the Stability of Casein Micelles*, Journal of Dairy Science, Elsevier, Vol. 73, No. 8, pp. 1965–1979.
- Wang, C., Kim, J., Jin, C.T., Leong, P.H.W. and McEwan, A. (2012) *Review: Near infrared spectroscopy in optical coherence tomography*, Journal of Near Infrared Spectroscopy, Vol. 20, No. 1, pp. 237–247.
- Welinder, K.G. (1988) *Generation of peptides suitable for sequence analysis by proteolytic cleavage in reversed-phase high-performance liquid chromatography solvents*, Analytical Biochemistry, Academic Press, Vol. 174, No. 1, pp. 54–64.
- Yang, C., Yu, C., Zhang, M., Yang, X., Dong, H., Dong, Q., Zhang, H., *et al.* (2022) *Investigation of protective effect of ethanol on the natural structure of protein with infrared spectroscopy*, Spectrochimica Acta Part A: Molecular and Biomolecular Spectroscopy, Elsevier, Vol. 271, pp. 120935.

Yoshikawa, H., Hirano, A., Arakawa, T. and Shiraki, K. (2012) *Effects of alcohol on the solubility and structure of native and disulfide-modified bovine serum albumin*, International Journal of Biological Macromolecules, Elsevier B.V., Vol. 50, No. 5, pp. 1286–1291.

